Salhab *EURASIP Journal on Wireless Communications and Networking* (2016) 2016:260
DOI 10.1186/s13638-016-0751-9

EURASIP Journal on Wireless Communications and Networking

RESEARCH Open Access

A new scenario of triple-hop mixed RF/FSO/RF relay network with generalized order user scheduling and power allocation

Anas M. Salhab

Abstract

This paper proposes and evaluates the performance of multiuser (MU) triple-hop mixed radio frequency (RF)/free-space optical (FSO) relay network with generalized order user scheduling. An important example on the applicability of this scenario is in cellular networks where two sets of various users are communicating with their own base stations (BSs) over RF links and these BSs are connected together via an FSO link. The considered system includes K_1 sources or users, two decode-and-forward (DF) relays, and K_2 destinations or users. The sources and destinations are connected with their relay nodes through RF links, and the relays are connected with each other through an FSO link. To achieve MU diversity, the generalized order user scheduling is used on the RF hops to select among sources and destinations. In the analysis, the RF channels are assumed to follow the Rayleigh fading model and the FSO channel is assumed to follow the Gamma-Gamma fading model including the effect of pointing errors. Closed-form expressions are derived for the outage probability, average symbol error probability (ASEP), and ergodic channel capacity. Moreover, in order to gain more insight onto the system behavior, the system is studied at the signal-to-noise ratio (SNR) regime whereby the diversity order and coding gain are provided and studied. The asymptotic results are used to obtain the optimum transmission power of the system. Monte Carlo simulations are given to validate the achieved exact and asymptotic results. The results show that the diversity order and coding of the proposed scenario are determined by the worst link among the three links. Also, results illustrate the effectiveness of the proposed power allocation algorithm in enhancing the system performance compared to the case with no power allocation.

Keywords: Mixed RF/FSO/RF relay network, Generalized order user scheduling, Multiuser diversity, Rayleigh fading, Gamma-Gamma fading, Power allocation

1 Introduction

The free-space optical (FSO) communication has been recently proposed as an efficient means to deal with the "last-mile" problem in wireless networks [1]. In such systems, the data transmission takes place between an optical transmitter and a receiver located, for example, on high buildings, separated by several hundred meters. Having the ability to operate on unlicensed optical beams and the potential for providing broadband communication capacity, the FSO communications represent a cost-effective alternative and/or a complement to radio frequency (RF) counterparts. In addition, features such as high security, flexibility, rapid deployment time, and rigidity to RF interference have made FSO communications appealing for emergency situation recovery and military applications [2].

Cooperative relay networks have recently attracted the attention of many researchers as an efficient solution for the multipath fading problem in wireless communications [3]. Using relays in wireless networks aims to provide diversity, widen the coverage area, and reduce the need for high-power transmitters. In such networks, a relay node or a set of relays help a source node in sending its message to the destination via either an amplify-and-forward (AF) scheme or a decode-and-forward (DF) scheme. Despite its requirement for more signal processing, the DF relaying protocol gives better results compared to the AF protocol, especially at low signal-to-noise ratio (SNR) values.

Correspondence: salhab@kfupm.edu.sa
[1]Electrical Engineering Department, King Fahd University of Petroleum and Minerals, 31261 Dhahran, Saudi Arabia

Recently, a mixture of relay and FSO networks has been introduced in the literature aiming to increase the coverage distance of FSO networks which is usually limited to a few hundred meters in realistic conditions due to atmospheric turbulence condition effects [4]. In such networks, the source message is transmitted to a relay node over an RF link and then forwarded to the destination over an FSO link. Having relays in wireless networks helps in increasing the communication distance as well as in providing diversity.

The new scenario of mixed RF/FSO relaying network can be also used for user multiplexing where multiple users with only RF capability can be multiplexed into a single FSO link [5]. The RF/FSO relay communication has the ability to fill the connectivity gap between the last-mile network and the backbone network as in developing countries where the last-mile connectivity can be delivered via high-speed FSO links [6]. Such mixed relaying scheme conserves economic resources by avoiding unnecessary modifications to the current mobile devices and, at the same time, saves bandwidth by utilizing FSO capabilities. These attractive features of mixed RF/FSO relay networks make them a strong candidate for current and soon-to-come wireless networks.

The FSO relaying networks with single relay have been studied in the literature under various conditions [7, 8]. The outage performance of AF and DF FSO relaying networks over log-normal fading channels was studied in [7] assuming the presence of a direct link between the source and the destination. The log-normal fading model is usually used to model the FSO links assuming weak atmospheric turbulence conditions, whereas the Gamma-Gamma fading model is more accurate and can be used to model the FSO links under both weak and strong turbulence conditions. The performance of FSO relay networks over Gamma-Gamma fading channels was studied in [8]. The exact outage and error probabilities of two-way FSO relay networks were derived in addition to the derivation of an approximate expression for the symbol error probability. The effect of pointing errors was combined with the turbulence-induced fading as one channel statistic in studying the performance of dual-hop mixed RF/FSO relay networks in [5].

In the area of parallel FSO relaying, the authors in [9, 10] studied the performance of dual-hop FSO networks over log-normal channels for DF and AF schemes, respectively. The performance of dual-hop FSO selective relaying network where the source message is forwarded to the destination along the direct link or along the best relay was studied in [11]. Closed-form and asymptotic expressions were derived for the bit error probability assuming Rayleigh and log-normal fading channels. A key paper which provides some new exact and approximate statistics of the sum of Gamma-Gamma variates and their application in RF and FSO DF relay networks was presented in [12]. The outage performance of channel state information (CSI)-assisted and semi-blind AF opportunistic FSO relay networks was studied in [13] assuming composite channels.

Recently, the scenario of mixed RF/FSO relay networks with multiple users has induced several researchers to turn their attention to work on this hot topic. In [5, 14], the outage and error probabilities in addition to channel capacity of dual-hop multiuser DF and fixed-gain AF mixed RF/FSO relay networks were derived and analyzed, respectively. Despite the presence of multiple users, only one user was assumed to communicate with a relay node through an RF link and the relay was assumed to be connected with a destination through a Gamma-Gamma-modeled FSO channel with pointing errors. No multiuser diversity was achieved in that study. In [15], Miridakis et al. studied the outage and error probability performance of multiuser dual-hop DF mixed RF/FSO relay network with the V-BLAST technique. A resource allocation scheme for multiuser mixed RF/FSO relay network was proposed in [16], where the data of users on the RF hop are generated according to a zero-mean rotationally invariant complex Gaussian distribution. The authors claimed the effectiveness of the proposed link allocation protocol even in the conditions where the FSO link is affected by severe atmospheric conditions. The area of hybrid RF-FSO networks has been recently of interest for many researchers. In [17], considering the cases with and without hybrid automatic repeat request (HARQ) and joint transmission and reception of the RF and FSO messages, the authors derived closed-form expressions for the message decoding probabilities, the throughput, and the outage probability of the RF-FSO setups. The same scenario was also studied by the same authors in [18] but with consideration to the effect of adaptive power allocation on the system throughput and outage probability.

Most recently, the performance of the multiuser mixed RF/FSO relay network with outdated channel information and power allocation has been presented in [19]. Opportunistic scheduling where the user of the best RF channel is selected to send its message to the relay node was used. A generalization to the work in [19] was considered in [20], where the user of the N^{th} best RF channel is selected to send its message to the relay node in the first communication phase. Closed-form expressions for the outage and symbol error probabilities were derived, in addition to channel capacity with the effect of outdate channel information. In [21], the security analysis of multiuser mixed RF/FSO relay networks was analyzed. The paper studied the effect of a single passive eavesdropper attack on the performance of mixed RF/FSO relay network with multiple users and multiple antennas relay. The RF links and FSO link were assumed to follow the Nakagami-*m* and Gamma-Gamma fading models, respectively, with consideration to the effect of pointing errors on the FSO link. The authors derived closed-form expressions for the outage probability, average symbol error probability (ASEP), and channel capacity as reliability performance measures for the authorized mixed RF/FSO relay network and closed-from expression for the intercept probability as a security measure. Asymptotic expressions were also derived for the outage probability at high SNR values and used for achieving the optimum transmission powers of the selected user and relay node, where opportunistic scheduling was used to select among the users of the first hop.

Most of the previous studies considered the scenario of the dual-hop mixed RF/FSO relay network. This scenario could be seen in applications where multiple users communicate with a relay node via RF links and the relay forwards their massages to a base station (BS) over an FSO link. Also, such a scenario can be seen in indoor applications where multiple users communicate with an access point that is in turn connected to a macro BS via an FSO link [16]. Another important scenario which can be seen in practice is the triple-hop mixed RF/FSO/RF relay network. Example of such applications are as follows: (1) in cellular networks where two sets of various users communicate with their own BSs over RF links and these BSs are connected together via an FSO link and (2) in indoor applications where two sets of users communicate with their access points inside two buildings and these access points are connected via an FSO link. The same setup of triple-hop relay network can be also used in other types of networks such as in mixed mmWave RF/FSO/mmWave RF relaying network, mixed RF/visible light communication (VLC)/RF relaying network, and mixed VLC/RF/VLC relaying network. To exploit the presence of multiple users and achieve the multiuser diversity in such networks, a single user can be selected/scheduled among the available users and allowed to conduct its transmission. The opportunistic scheduling is among the well-known and efficient user selection schemes that are usually used to select among the users. In this scheme, the user with the best channel is always allowed to conduct its transmission in a downlink or an uplink scenario. Also, this scheme is usually used to achieve the maximum sum-rate capacity in wireless networks. A generalization to the opportunistic user scheduling is the generalized order user scheduling, where the user of the N^{th} best channel is selected for conducting its communication. This scheme is applicable in situations where the scheduling unit fails in error in selecting the best user among the available users due to error in estimating the users' channels. More papers can be found in the literature on mixed or hybrid networks with and without relay nodes [22–24]. Also, it is worthwhile to mention here that the scenario of triple-hop relaying was already considered in literature by many researchers but for one type of links [25, 26].

In this paper, we introduce the new scenario of triple-hop mixed RF/FSO/RF relay network with the generalized order user scheduling scheme to select among the users of the first and third RF links. The considered system includes K_1 sources or users, two DF relays, and K_2 destinations. The sources and destinations are connected with their relay nodes through the RF links, and the relays are connected with each other through an FSO link. Using the generalized order user scheduler, the source with the N_1^{th} best SNR among the available sources is allowed to communicate with the first relay node. Also, using the same scheduling criterion, the destination which has the N_2^{th} best SNR is selected to receive its message from the second relay. Furthermore, the RF links are assumed to follow the Rayleigh fading model and the FSO link is assumed to follow the Gamma-Gamma fading model with the effect of pointing errors. Closed-form expressions are derived for the outage probability, ASEP, and ergodic channel capacity. Moreover, the system performance is studied at the high SNR regime, where approximate expressions for the outage probability, the diversity order, and coding gain are derived and analyzed. Furthermore, the asymptotic results are used to obtain the optimum transmission powers of the selected user on the first hop, the first relay, and the second relay. Some simulation and numerical examples are provided to study the effect of the number of users and order of selected users on both the first and third hops, atmospheric turbulence parameters, pointing errors, and power allocation on the system performance.

The rest of this paper is organized as follows. Section 2 presents the system and channel models. The exact performance analysis is evaluated in Section 3. Section 4 provides the asymptotic outage performance analysis and power allocation. Some simulation and numerical results are presented and discussed in Section 5. Finally, conclusions are given in Section 6.

2 System and channel models

Consider a triple-hop mixed RF/FSO/RF relay network consisted of K_1 sources on the first hop U_k $(k = 1, \ldots, K_1)$, two un-coded type DF relays R_i $(i = 1, 2)$, and K_2 destinations on the third hop D_j $(j = 1, \ldots, K_2)$, as shown in Fig. 1. The sources are assumed to be connected with the first relay node through RF links; this relay is connected with another relay through an FSO link, and finally, the second relay is connected with the destinations through RF links. It is assumed that each user is equipped with a single antenna: the first relay is equipped with a single antenna and a single photo-aperture transmitter; the second relay is equipped with a single photo detector and a single antenna, and each destination is equipped with a single antenna. The direct links between the sources

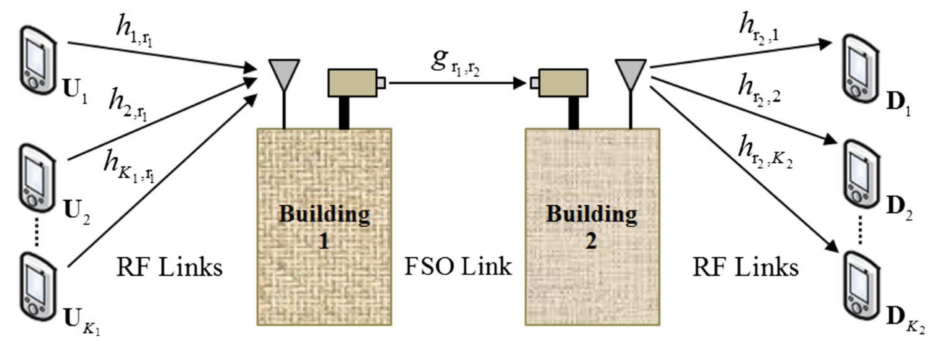

Fig. 1 Multiuser triple-hop mixed RF/FSO/RF relay network with generalized order user scheduling

and destinations are assumed to be in deep fade, and hence, they are not considered in the analysis of this paper. Also, we assume block fading model where the channel coefficient stays constant over an entire block of communication. The communication is assumed to operate in a half-duplex mode and to be conducted over three phases: selected user $\mathsf{U}_{\mathrm{Sel}} \to \mathsf{R}_1$, $\mathsf{R}_1 \to \mathsf{R}_2$, and $\mathsf{R}_2 \to \mathsf{D}_{\mathrm{Sel}}$. The received signal at R_1 from the kth user can be expressed as

$$y_{k,\mathrm{r}_1} = \sqrt{P_k} h_{k,\mathrm{r}_1} x_{k,\mathrm{r}_1} + n_{\mathrm{r}_1}, \tag{1}$$

where P_k is the transmit power of the kth user, h_{k,r_1} is the channel coefficient of the $\mathsf{U}_k \to \mathsf{R}_1$ link, x_{k,r_1} is the transmitted symbol of U_k with $\mathbb{E}\{|x_{k,\mathrm{r}_1}|^2\} = 1$, and $n_{\mathrm{r}_1} \sim \mathcal{N}(0, N_{01})$ is an additive white Gaussian noise (AWGN) term, where $\mathbb{E}\{\cdot\}$ is the mathematical expectation.

Using (1), the SNR at R_1 due to U_k can be written as

$$\gamma_{\mathsf{U}_k,\mathsf{R}_1} = \frac{P_k}{N_{01}} |h_{k,\mathrm{r}_1}|^2. \tag{2}$$

According to the generalized order user scheduling, the source with the N_1^{th} best $\gamma_{\mathsf{U}_k,\mathsf{R}_1}$ or equivalently, the N_1^{th} largest $|h_{k,\mathrm{r}_1}|^2$ among the other sources is selected to transmit its message to R_1 in the first communication phase. In other words, the source is selected such that $\gamma_{\mathsf{U}_{\mathrm{Sel}},\mathsf{R}_1} = N_1^{\mathrm{th}} \max_k \left\{\gamma_{\mathsf{U}_k,\mathsf{R}_1}\right\}$. The subcarrier intensity modulation (SIM) scheme is employed at the relay R_1, where a standard RF coherent/noncoherent modulator and demodulator can be used for transmitting and recovering the source data [27–29]. At R_1, after filtering by a bandpass filter (BPF), a direct current (DC) bias is added to the filtered RF signal to ensure that the optical signal is non-negative. Then, the biased signal is sent to a continuous wave laser driver. The retransmitted optical signal at R_1 is written as [4]

$$y_{\mathrm{r}_1}^{\mathrm{Opt}} = \sqrt{P_{\mathrm{Opt}}}(1 + \mathcal{M} y_{\mathrm{Sel},\mathrm{r}_1}), \tag{3}$$

where P_{Opt} denotes the average transmitted optical power and it is related to the relay electrical power P_{r} by the electrical-to-optical conversion efficiency η_1 as $P_{\mathrm{Opt}} = \eta_1 P_{\mathrm{r}_1}$, $\mathcal{M}$ denotes the modulation index, and $y_{\mathrm{Sel},\mathrm{r}_1}$ is the RF received signal at R_1 from the selected source. The optical signal at R_2 received from R_1 at the second phase of communication can be expressed as

$$y_{\mathrm{r}_1,\mathrm{r}_2} = g_{\mathrm{r}_1,\mathrm{r}_2} \left\{ \sqrt{P_{\mathrm{Opt}}} \left[1 + \mathcal{M} \left(\sqrt{P_{\mathrm{Sel}}} h_{\mathrm{Sel},\mathrm{r}_1} x_{\mathrm{Sel},\mathrm{r}_1} + n_{\mathrm{r}_1} \right) \right] \right\} + n_{\mathrm{r}_2}, \tag{4}$$

where $n_{\mathrm{r}_2} \sim \mathcal{N}(0, N_{02})$ is an AWGN term at R_2. Moreover, the channel coefficient of the $\mathsf{R}_1 \to \mathsf{R}_2$ link which is given by $g_{\mathrm{r}_1,\mathrm{r}_2}$ is modeled as $g_{\mathrm{r}_1,\mathrm{r}_2} = g_a g_f$, where g_a and g_f are the average gain and the fading gain of the FSO link, respectively, and are given by [30]

$$\begin{cases} g_a = \left[\mathrm{erf}\left(\frac{\sqrt{\pi} q}{\sqrt{2}\phi d^{\mathrm{FSO}}} \right) \right]^2 \times 10^{-\kappa d^{\mathrm{FSO}}/10}, \\ g_f \sim \mathrm{GGamma}(\alpha, \beta), \end{cases} \tag{5}$$

where q is the aperture radius, ϕ is the divergence angle of the beam, d^{FSO} is the distance between the FSO transmitter and the receiver, κ is the weather-dependent attenuation coefficient, and $\mathrm{GGamma}(\alpha, \beta)$ represents a Gamma-Gamma random variable with parameters α and β. Assuming spherical wave propagation, the parameters α and β in the Gamma-Gamma distribution which represent the fading turbulence conditions are related to the physical parameters as follows [31]:

$$\alpha = \left[\exp\left\{ \frac{0.49\vartheta^2}{\left[1 + 0.18\xi^2 + 0.56\vartheta^{12/5}\right]^{7/6}} \right\} - 1 \right]^{-1}, \tag{6}$$

$$\beta = \left[\exp\left\{ \frac{0.51\vartheta^2 [1 + 0.69\vartheta^{12/5}]^{-5/6}}{\left[1 + 0.9\xi^2 + 0.62\xi^2\vartheta^{12/5}\right]^{5/6}} \right\} - 1 \right]^{-1}, \tag{7}$$

where $\vartheta^2 = 0.5 C_n^2 \varsigma^{7/6} (d^{\mathrm{FSO}})^{11/6}$, $\xi^2 = \varsigma q^2 / d^{\mathrm{FSO}}$, and $\varsigma = 2\pi/\lambda^{\mathrm{FSO}}$. Here, λ^{FSO} is the wavelength and C_n^2 is the weather-dependent index of refraction structure parameter.

When the DC component is filtered out at R_2 and an optical-to-electrical conversion is performed and assuming $\mathcal{M} = 1$, the received signal can be expressed as follows:

$$y_{\mathsf{r}_1,\mathsf{r}_2} = g_{\mathsf{r}_1,\mathsf{r}_2}\sqrt{P_{\text{Ele}}}\left(\sqrt{P_{\text{Sel}}}h_{\text{Sel},\mathsf{r}_1}x_{\text{Sel},\mathsf{r}_2} + n_{\mathsf{r}_1}\right) + n_{\mathsf{r}_2}, \quad (8)$$

where $P_{\text{Ele}} = \eta_2 P_{\text{Opt}} = \eta_1\eta_2 P_{\mathsf{r}_1}$ is the electrical power received at R_2 with η_2 is the optical-to-electrical conversion efficiency.

From (8), the SNR at R_2 can be written as

$$\gamma_{\mathsf{R}_2} = \frac{\gamma_{\mathsf{U}_{\text{Sel}},\mathsf{R}_1}\gamma_{\mathsf{R}_1,\mathsf{R}_2}}{\gamma_{\text{Sel},\mathsf{R}_1} + \gamma_{\mathsf{R}_1,\mathsf{R}_2} + 1}, \quad (9)$$

where $\gamma_{\mathsf{U}_{\text{Sel}},\mathsf{R}_1} = \frac{P_{\text{Sel}}}{N_{01}}|h_{\text{Sel},\mathsf{r}_1}|^2$ and $\gamma_{\mathsf{R}_1,\mathsf{R}_2} = \frac{\eta_1\eta_2 P_{\mathsf{r}_1}}{N_{02}}|g_{\mathsf{r}_1,\mathsf{r}_2}|^2$, where P_{r_1} is the transmit power at R_1.

The SNR in (9) can be rewritten using the standard approximation $\gamma_{\mathsf{R}_2} \cong \min(\gamma_{\mathsf{U}_{\text{Sel}},\mathsf{R}_1}, \gamma_{\mathsf{R}_1,\mathsf{R}_2})$ as [5, 14]

$$\gamma_{\mathsf{R}_2} = \frac{\gamma_{\mathsf{U}_{\text{Sel}},\mathsf{R}_1}\gamma_{\mathsf{R}_1,\mathsf{R}_2}}{\gamma_{\mathsf{U}_{\text{Sel}},\mathsf{R}_1} + \gamma_{\mathsf{R}_1,\mathsf{R}_2}}. \quad (10)$$

The signal received at D_j from R_2 in the third phase of communication can be written as

$$y_{\mathsf{r}_2,\mathsf{d}_j} = \sqrt{P_{\mathsf{r}_2}}h_{\mathsf{r}_2,j}x_{\mathsf{d}_j} + n_{\mathsf{d}_j}, \quad (11)$$

where P_{r_2} is the transmit power at R_2, $h_{\mathsf{r}_2,j}$ is the channel coefficient of the $\mathsf{R}_2 \to \mathsf{D}_j$ link, x_{d_j} is the transmitted symbol of d_j with $\mathbb{E}\{|x_{\mathsf{d}_j}|^2\} = 1$, and $n_{\mathsf{d}_j} \sim \mathcal{N}(0, N_{03})$ is an AWGN term.

Using (11), the SNR at D_j can be written as

$$\gamma_{\mathsf{R}_2,\mathsf{D}_j} = \frac{P_{\mathsf{r}_2}}{N_{03}}|h_{\mathsf{r}_2,j}|^2. \quad (12)$$

According to the generalized order user scheduling, the destination with the N_2^{th} best $\gamma_{\mathsf{R}_2,\mathsf{D}_j}$ or equivalently, the N_2^{th} largest $|h_{\mathsf{r}_2,j}|^2$ among the other destinations is selected to receive its message from R_2 in the third communication phase. In other words, the destination is selected such that $\gamma_{\mathsf{R}_2,\mathsf{D}_{\text{Sel}}} = N_2^{\text{th}} \max_j \left\{\gamma_{\mathsf{R}_2,\mathsf{D}_j}\right\}$.

We assume that the channel coefficients of the RF links h_{k,r_1} ($k = 1 = \cdots = K_1$) and $h_{\mathsf{r}_2,j}$ ($j = 1 = \cdots = K_2$) follow the Rayleigh fading model and hence, the channel gains $|h_{k,\mathsf{r}_1}|^2$ and $|h_{\mathsf{r}_2,j}|^2$ are exponential distributed random variables with mean powers Ω_{k,r_1} and $\Omega_{\mathsf{r}_2,j}$, respectively. Therefore, the probability density functions (PDFs) of $\gamma_{\mathsf{U}_k,\mathsf{R}_1}$ and $\gamma_{\mathsf{R}_2,\mathsf{D}_j}$ are, respectively, given by $f_{\gamma_{\mathsf{U}_k,\mathsf{R}_1}}(\gamma) = \lambda_{k,\mathsf{r}_1}\exp\left(-\lambda_{k,\mathsf{r}_1}\gamma\right)$, where $\lambda_{k,\mathsf{r}_1} = 1/\bar{\gamma}_{k,\mathsf{r}_1}$ with $\bar{\gamma}_{k,\mathsf{r}_1} = \frac{P_k}{N_0}\mathbb{E}\{|h_{k,\mathsf{r}_1}|^2\} = \frac{P_k}{N_{01}}\Omega_{k,\mathsf{r}_1}$ and $f_{\gamma_{\mathsf{R}_2,\mathsf{D}_j}}(\gamma) = \lambda_{\mathsf{r}_2,j}\exp\left(-\lambda_{\mathsf{r}_2,j}\gamma\right)$, where $\lambda_{\mathsf{r}_2,j} = 1/\bar{\gamma}_{\mathsf{r}_2,j}$ with $\bar{\gamma}_{\mathsf{r}_2,j} = \frac{P_k}{N_{03}}\mathbb{E}\{|h_{\mathsf{r}_2,j}|^2\} = \frac{P_{\mathsf{r}_2}}{N_{03}}\Omega_{\mathsf{r}_2,j}$. On the other hand, it is assumed that the FSO link experiences a unified Gamma-Gamma fading model including the pointing errors effect whose SNR PDF is given by [5]

$$f_{\gamma_{\mathsf{R}_1,\mathsf{R}_2}}(\gamma) = \frac{\zeta^2}{r\gamma\Gamma(\alpha)\Gamma(\beta)}\mathrm{G}_{1,3}^{3,0}\left[\alpha\beta\left(\lambda_{\mathsf{r}_1,\mathsf{r}_2}\gamma\right)^{\frac{1}{r}}\,\middle|\,\begin{matrix}\zeta^2+1\\ \zeta^2,\alpha,\beta\end{matrix}\right], \quad (13)$$

where ζ is the ratio between the equivalent beam radius at the receiver and the pointing error displacement standard deviation (jitter) at the receiver (i.e. when $\zeta \to \infty$, we get the non-pointing error case) [5], r is the parameter defining the type of detection technique (i.e. $r = 1$ represents heterodyne detection and $r = 2$ represents intensity modulation (IM)/direct detection (DD)), α and β are the fading parameters related to the atmospheric turbulence conditions with lower values indicating severe atmospheric turbulence conditions, $\Gamma(.)$ is the Gamma function as defined in [32, Eq. (8.310)], $\lambda_{\mathsf{r}_1,\mathsf{r}_2} = 1/\bar{\gamma}_{\mathsf{r}_1,\mathsf{r}_2}$ with $\bar{\gamma}_{\mathsf{r}_1,\mathsf{r}_2} = \frac{\eta_1\eta_2 P_{\mathsf{r}_1}}{N_{02}}\mathbb{E}\{|g_{\mathsf{r}_1,\mathsf{r}_2}|^2\} = \frac{\eta_1\eta_2 P_{\mathsf{r}_1}}{N_{02}}\mu_{\mathsf{r}_1,\mathsf{r}_2}$, and G(.) is the Meijer G-function as defined in [32, Eq. (9.301)].

The end-to-end (e2e) SNR at the selected destination can be written using the standard approximation $\gamma_{\mathsf{D}} \cong \min(\gamma_{\mathsf{R}_2}, \gamma_{\mathsf{R}_2,\mathsf{D}_{\text{Sel}}})$ as [5, 14]

$$\gamma_{\mathsf{D}} = \frac{\gamma_{\mathsf{R}_2}\gamma_{\mathsf{R}_2,\mathsf{D}_{\text{Sel}}}}{\gamma_{\mathsf{R}_2} + \gamma_{\mathsf{R}_2,\mathsf{D}_{\text{Sel}}}}. \quad (14)$$

Achieving the system performance measures requires obtaining the statistics of the e2e SNR provided in (14).

3 Exact performance analysis

In this section, we derive the exact outage probability, ASEP, and channel capacity of the considered system.

3.1 Outage probability

The outage probability is an important performance metric in wireless communications and defined as the probability that the SNR at the selected destination goes below a predetermined outage threshold γ_{out}, i.e., $P_{\text{out}} = \Pr\left[\gamma_{\mathsf{D}} \le \gamma_{\text{out}}\right]$, where $\Pr[\,.]$ is the probability operation and γ_{out} is a predetermined outage threshold or, equivalently, the system is unable to achieve adequate reception which is common to occur in any communication system. The outage probability is also equivalent to other metrics which is the outage capacity (different way of looking into the system quality), where for any given rate and outage probability level, there is an outage capacity associated with it, with the interpretation that when the system is not in outage (which occurs with probability $1 - P_{\text{out}}$), this particular transmission rate can be supported [33]. Clearly, the outage probability can be obtained from the cumulative distribution function (CDF) of the e2e SNR as

$P_{\text{out}} = F_{\gamma_{\text{D}}}(\gamma_{\text{out}})$. This CDF can be written in terms of CDFs of the three hops' SNRs as [34]

$$F_{\gamma_{\text{D}}}(\gamma) = 1 - \left\{ \left(1 - F_{\gamma_{\text{U}_{\text{Sel}},\text{R}_1}}(\gamma)\right)\left(1 - F_{\gamma_{\text{R}_1,\text{R}_2}}(\gamma)\right) \times \left(1 - F_{\gamma_{\text{R}_2,\text{D}_{\text{Sel}}}}(\gamma)\right)\right\}, \quad (15)$$

where $F_{\gamma_{\text{U}_{\text{Sel}},\text{R}_1}}(\gamma)$, $F_{\gamma_{\text{R}_1,\text{R}_2}}(\gamma)$, and $F_{\gamma_{\text{R}_2,\text{D}_{\text{Sel}}}}(\gamma)$ are the CDFs of first hop, second hop, and third hop SNRs, respectively. It is clear from (15) that the system gets in outage once at least one of the three hops gets in outage or, equivalently, the SNR of that hop becomes less than γ_{out}. With a direct expansion, the CDF in (15) can be rewritten in a more detailed form as follows:

$$\begin{aligned} F_{\gamma_{\text{D}}}(\gamma) = & F_{\gamma_{\text{U}_{\text{Sel}},\text{R}_1}}(\gamma) + F_{\gamma_{\text{R}_1,\text{R}_2}}(\gamma) + F_{\gamma_{\text{R}_2,\text{D}_{\text{Sel}}}}(\gamma) \\ & - F_{\gamma_{\text{U}_{\text{Sel}},\text{R}_1}}(\gamma)F_{\gamma_{\text{R}_1,\text{R}_2}}(\gamma) - F_{\gamma_{\text{U}_{\text{Sel}},\text{R}_1}}(\gamma)F_{\gamma_{\text{R}_2,\text{D}_{\text{Sel}}}}(\gamma) \\ & - F_{\gamma_{\text{R}_1,\text{R}_2}}(\gamma)F_{\gamma_{\text{R}_2,\text{D}_{\text{Sel}}}}(\gamma) + F_{\gamma_{\text{U}_{\text{Sel}},\text{R}_1}}(\gamma)F_{\gamma_{\text{R}_1,\text{R}_2}}(\gamma) \\ & \times F_{\gamma_{\text{R}_2,\text{D}_{\text{Sel}}}}(\gamma). \end{aligned} \quad (16)$$

In order to calculate (16), the CDF of each hop of the three hops needs to be obtained first as follows.

1. First hop link
   Using the generalized order user selection, the PDF $f_{\gamma_{\text{U}_{\text{Sel}},\text{R}_1}}(\gamma)$ can be written for independent identically distributed sources' channels ($\lambda_{1,\text{r}_1} = \lambda_{2,\text{r}_1} = \ldots = \lambda_{K_1,\text{r}_1} = \lambda_{u,\text{r}_1}$) as [35]

$$f_{\gamma_{\text{U}_{\text{Sel}},\text{R}_1}}(\gamma) = \binom{K_1 - 1}{N_1 - 1} K_1 f_{\gamma_{\text{U},\text{R}_1}}(\gamma)\left(F_{\gamma_{\text{U},\text{R}_1}}(\gamma)\right)^{K_1 - N_1} \times \left(1 - F_{\gamma_{\text{U},\text{R}_1}}(\gamma)\right)^{N_1 - 1}, \quad (17)$$

   where $f_{\gamma_{\text{U},\text{R}_1}}(\gamma)$ and $F_{\gamma_{\text{U},\text{R}_1}}(\gamma)$ are the PDF and CDF of a source channel's SNR at the first hop, respectively, which are given for the Rayleigh fading channels by $f_{\gamma_{\text{U},\text{R}_1}}(\gamma) = \lambda_{u,\text{r}_1} \exp\left(-\lambda_{u,\text{r}_1}\gamma\right)$ and $F_{\gamma_{\text{U},\text{R}_1}}(\gamma) = 1 - \exp\left(-\lambda_{u,\text{r}_1}\gamma\right)$, and N_1 is the order of the selected source. In other words, the PDF in (17) represents the PDF of the N_1^{th} best SNR or, equivalently, the source of the best N_1^{th} SNR is selected by the first relay.
   Upon substituting these statistics in (17) and using the binomial rule, the PDF in (17) can be rewritten as

$$f_{\gamma_{\text{U}_{\text{Sel}},\text{R}_1}}(\gamma) = K_1 \lambda_{u,\text{r}_1} \binom{K_1 - 1}{N_1 - 1} \sum_{k=0}^{K_1 - N_1} \binom{K_1 - N_1}{k} \times (-1)^k \exp\left(-(k + N_1)\lambda_{u,\text{r}_1}\gamma\right). \quad (18)$$

   Integrating, (18) using $\int_0^\gamma f_{\gamma_{\text{U}_{\text{Sel}},\text{R}_1}}(t)dt$, we get

$$F_{\gamma_{\text{U}_{\text{Sel}},\text{R}_1}}(\gamma) = K_1 \binom{K_1 - 1}{N_1 - 1} \sum_{k=0}^{K_1 - N_1} \frac{\binom{K_1 - N_1}{k}(-1)^k}{(k + N_1)} \times \left[1 - \exp\left(-(k + N_1)\lambda_{u,\text{r}_1}\gamma\right)\right]. \quad (19)$$

2. Second hop link
   The CDF $F_{\gamma_{\text{R}_1,\text{R}_2}}(\gamma)$ can be obtained by integrating the PDF in (13) using $\int_0^\gamma f_{\gamma_{\text{R}_1,\text{R}_2}}(t)dt$ and with the help of Eq. 07.34.21.0003.01 in [36] to get

$$F_{\gamma_{\text{R}_1,\text{R}_2}}(\gamma) = A G_{r+1,3r+1}^{3r,1}\left[\frac{B}{\bar{\gamma}_{\text{r}_1,\text{r}_2}}\gamma \,\middle|\, \begin{matrix} 1, \chi_1 \\ \chi_2, 0 \end{matrix}\right], \quad (20)$$

   where $A = \frac{r^{\alpha+\beta-2}\zeta^2}{(2\pi)^{r-1}\Gamma(\alpha)\Gamma(\beta)}$, $B = \frac{(\alpha\beta)^r}{r^{2r}}$, $\chi_1 = \frac{\zeta^2+1}{r}, \ldots, \frac{\zeta^2+r}{r}$ comprises of r terms, and $\chi_2 = \frac{\zeta^2}{r}, \ldots, \frac{\zeta^2+r-1}{r}, \frac{\alpha}{r}, \ldots, \frac{\alpha+r-1}{r}, \frac{\beta}{r}, \ldots, \frac{\beta+r-1}{r}$ comprises of $3r$ terms. Note that introducing these parameters primarily aims to simplify the calculations and expressions of the paper.
3. Third hop link
   Similar to the first hop link, the PDF and CDF of the SNR of the selected destination can be, respectively, written as

$$f_{\gamma_{\text{R}_2,\text{D}_{\text{Sel}}}}(\gamma) = K_2 \lambda_{\text{r}_2,u} \binom{K_2 - 1}{N_2 - 1} \sum_{j=0}^{K_2 - N_2} \binom{K_1 - N_1}{j} \times (-1)^j \exp\left(-\left(j + N_2\right)\lambda_{\text{r}_2,u}\gamma\right), \quad (21)$$

$$F_{\gamma_{\text{R}_2,\text{D}_{\text{Sel}}}}(\gamma) = K_2 \binom{K_2 - 1}{N_2 - 1} \sum_{j=0}^{K_2 - N_2} \frac{\binom{K_2 - N_2}{j}(-1)^j}{\left(j + N_2\right)} \times \left[1 - \exp\left(-\left(j + N_2\right)\lambda_{\text{r}_2,u}\gamma\right)\right], \quad (22)$$

   where the users on the third hop have been assumed to have independent identical distributed channels in (21) and (22), that is, ($\lambda_{\text{r}_2,1} = \lambda_{\text{r}_2,2} = \ldots = \lambda_{\text{r}_2,K_2} = \lambda_{\text{r}_2,u}$). Again, the PDF in (21) represents the PDF of the N_2^{th} best SNR or, equivalently, that the destination of the N_2^{th} best SNR is selected by the second relay.

Upon substituting (19), (20), and (22) in (15) and after some simplifications, we get

$$
\begin{aligned}
F_{\gamma_{\rm D}}(\gamma) =& \binom{K_1-1}{N_1-1}K_1 \sum_{k=0}^{K_1-N_1} \frac{\binom{K_1-N_1}{k}(-1)^k}{(k+N_1)} \Bigg\{1-\exp\left(-\tau_1\gamma\right) - A \\
&\times \left(\mathrm{G}_{r+1,3r+1}^{3r,1}\left[\delta_0\gamma \left| \begin{matrix} 1,\chi_1 \\ \chi_2,0 \end{matrix}\right.\right] \left[1-\exp\left(-\tau_1\gamma\right)\right]\right)\Bigg\} \\
&+ \binom{K_2-1}{N_2-1}K_2 \sum_{j=0}^{K_2-N_2} \frac{\binom{K_2-N_2}{j}(-1)^j}{(j+N_2)} \Bigg\{1-\exp\left(-\tau_2\gamma\right) \\
&-A\left(\mathrm{G}_{r+1,3r+1}^{3r,1}\left[\delta_0\gamma \left| \begin{matrix} 1,\chi_1 \\ \chi_2,0 \end{matrix}\right.\right] \left[1-\exp\left(-\tau_2\gamma\right)\right]\right)\Bigg\} \\
&- \binom{K_1-1}{N_1-1}K_1 \sum_{k=0}^{K_1-N_1} \frac{\binom{K_1-N_1}{k}(-1)^k}{(k+N_1)} \binom{K_2-1}{N_2-1}K_2 \\
&\times \sum_{j=0}^{K_2-N_2} \frac{\binom{K_2-N_2}{j}(-1)^j}{(j+N_2)} \Bigg\{1-\exp\left(-\tau_1\gamma\right) - \exp\left(-\tau_2\gamma\right) \\
&+\exp\left(-\left[\tau_1+\tau_2\right]\gamma\right) - A\Bigg(\mathrm{G}_{r+1,3r+1}^{3r,1}\left[\delta_0\gamma \left| \begin{matrix} 1,\chi_1 \\ \chi_2,0 \end{matrix}\right.\right] \\
&\times\left[1-\exp\left(-\tau_1\gamma\right)-\exp\left(-\tau_2\gamma\right)+\exp\left(-\left[\tau_1+\tau_2\right]\gamma\right)\right]\Bigg)\Bigg\} \\
&+ A\mathrm{G}_{r+1,3r+1}^{3r,1}\left[\delta_0\gamma \left| \begin{matrix} 1,\chi_1 \\ \chi_2,0 \end{matrix}\right.\right],
\end{aligned}
\tag{23}
$$

where $\tau_1 = (k+N_1)\lambda_{u,\mathrm{r}_1}$, $\delta_0 = \frac{B}{\bar{\gamma}_{\mathrm{r}_1,\mathrm{r}_2}}$, and $\tau_2 = (j+N_2)\lambda_{\mathrm{r}_2,u}$.

The CDF in (23) represents an important statistic to the e2e SNR $\gamma_{\rm D}$ and allows to derive several performance measures in closed-form expressions as will be seen in the next sections of the paper. Up to now, the outage probability can be obtained by replacing γ by $\gamma_{\rm out}$ in (23).

3.2 Average symbol error probability

For evaluating the ASEP, we use the CDF-based method where the ASEP can be expressed in terms of the CDF of $\gamma_{\rm D}$ as [37]

$$
\mathrm{ASEP} = \frac{a\sqrt{b}}{2\sqrt{\pi}} \int_0^{\infty} \frac{\exp\left(-b\gamma\right)}{\sqrt{\gamma}} F_{\gamma_{\rm D}}(\gamma) d\gamma, \tag{24}
$$

where a and b are modulation-specific parameters. Note that we adopt the SIM scheme and hence the known digital modulation techniques can be used, such as phase shift keying (PSK) [38]. Therefore, the error probability computing method (24) used in RF wireless communication systems can be used to evaluate the error probability performance in FSO systems.

Upon substituting (23) in (24) and using Eq. 7.813.1 in [32] and Eq. 3.381.4 in [32], we get

$$
\begin{aligned}
\mathrm{ASEP} =& \frac{a\sqrt{b}}{2\sqrt{\pi}} \Bigg\{ \binom{K_1-1}{N_1-1}K_1 \sum_{k=0}^{K_1-N_1} \frac{\binom{K_1-N_1}{k}(-1)^k}{(k+N_1)} \Bigg(\frac{\Gamma(1/2)}{b^{\frac{1}{2}}} \\
&- \frac{\Gamma(1/2)}{(b+\tau_1)^{\frac{1}{2}}} - A\Bigg[b^{-\frac{1}{2}}\mathrm{G}_{r+2,3r+1}^{3r,2}\left[\frac{\delta_0}{b} \left| \begin{matrix} \frac{1}{2},1,\chi_1 \\ \chi_2,0 \end{matrix}\right.\right] \\
&- (b+\tau_1)^{-\frac{1}{2}}\mathrm{G}_{r+2,3r+1}^{3r,2}\left[\frac{\delta_1}{(b+\tau_1)} \left| \begin{matrix} \frac{1}{2},1,\chi_1 \\ \chi_2,0 \end{matrix}\right.\right]\Bigg]\Bigg) + \binom{K_2-1}{N_2-1} \\
&\times K_2 \sum_{j=0}^{K_2-N_2} \frac{\binom{K_2-N_2}{j}(-1)^j}{(j+N_2)} \Bigg(\frac{\Gamma(1/2)}{b^{\frac{1}{2}}} - \frac{\Gamma(1/2)}{(b+\tau_2)^{\frac{1}{2}}} \\
&- A\Bigg[b^{-\frac{1}{2}}\mathrm{G}_{r+2,3r+1}^{3r,2}\left[\frac{\delta_0}{b} \left| \begin{matrix} \frac{1}{2},1,\chi_1 \\ \chi_2,0 \end{matrix}\right.\right] - (b+\tau_2)^{-\frac{1}{2}}\mathrm{G}_{r+2,3r+1}^{3r,2} \\
&\times \left[\frac{\delta_0}{(b+\tau_2)} \left| \begin{matrix} \frac{1}{2},1,\chi_1 \\ \chi_2,0 \end{matrix}\right.\right]\Bigg]\Bigg) - \binom{K_1-1}{N_1-1}K_1 \sum_{k=0}^{K_1-N_1} \frac{\binom{K_1-N_1}{k}}{(k+N_1)} \\
&\times (-1)^k \binom{K_2-1}{N_2-1}K_2 \sum_{j=0}^{K_2-N_2} \frac{\binom{K_2-N_2}{j}(-1)^j}{(j+N_2)} \Bigg(\frac{\Gamma(1/2)}{b^{\frac{1}{2}}} \\
&- \frac{\Gamma(1/2)}{(b+\tau_1)^{\frac{1}{2}}} - \frac{\Gamma(1/2)}{(b+\tau_2)^{\frac{1}{2}}} + \frac{\Gamma(1/2)}{(b+\tau_1+\tau_2)^{\frac{1}{2}}} \\
&- A\Bigg[b^{-\frac{1}{2}} \times \mathrm{G}_{r+2,3r+1}^{3r,2}\left[\frac{\delta_0}{b} \left| \begin{matrix} \frac{1}{2},1,\chi_1 \\ \chi_2,0 \end{matrix}\right.\right] - (b+\tau_1)^{-\frac{1}{2}}\mathrm{G}_{r+2,3r+1}^{3r,2} \\
&\times \left[\frac{\delta_0}{(b+\tau_1)} \left| \begin{matrix} \frac{1}{2},1,\chi_1 \\ \chi_2,0 \end{matrix}\right.\right] - \mathrm{G}_{r+2,3r+1}^{3r,2}\left[\frac{\delta_0}{(b+\tau_2)} \left| \begin{matrix} \frac{1}{2},1,\chi_1 \\ \chi_2,0 \end{matrix}\right.\right] \\
&\times (b+\tau_2)^{-\frac{1}{2}} + \mathrm{G}_{r+2,3r+1}^{3r,2}\left[\frac{\delta_0}{(b+\tau_1+\tau_2)} \left| \begin{matrix} \frac{1}{2},1,\chi_1 \\ \chi_2,0 \end{matrix}\right.\right] \\
&\times \left(b+\tau_1+\tau_2\right)^{-\frac{1}{2}}\Bigg]\Bigg) + Ab^{-\frac{1}{2}}\mathrm{G}_{r+2,3r+1}^{3r,2}\left[\frac{\delta_0}{b} \left| \begin{matrix} \frac{1}{2},1,\chi_1 \\ \chi_2,0 \end{matrix}\right.\right]\Bigg\}.
\end{aligned}
\tag{25}
$$

3.3 Ergodic channel capacity

It is well known that the atmospheric turbulence over the FSO links is slow in fading and since the coherence time of the channel is in the order of milliseconds (ms), the turbulence-induced fading remains constant over a large number of transmitted bits [39]. Furthermore, including the effects of the pointing error in our paper makes the signal fluctuate at a very high rate. Because the coherence time of the FSO fading channel is in the order of milliseconds, a single fade can obliterate millions of bits at gigabits/second data rates and therefore, the average (i.e., ergodic) capacity of the channel represents the best achievable capacity of an optical wireless link which is our focus in this work to ensure the long-term ergodic properties of the turbulence process [40]. Using the PDF-based method, the ergodic capacity can be expressed in terms of the PDF of γ_D as

$$C = \frac{1}{\ln(2)} \int_0^\infty \ln(1+\gamma) f_{\gamma_D}(\gamma) d\gamma. \tag{26}$$

It is clear that evaluating (26) requires the evaluation of $f_{\gamma_D}(\gamma)$ first. Upon differentiating (23) with respect to γ and using Eq. 07.34.20.0001.01 in [36], we get the following:

$$\begin{aligned} f_{\gamma_D}(\gamma) = & \binom{K_1-1}{N_1-1} K_1 \sum_{k=0}^{K_1-N_1} \frac{\binom{K_1-N_1}{k}(-1)^k}{\tau_1} \Bigg(\tau_1 \exp(-\tau_1\gamma) \\ & - A \left\{ \frac{1}{\delta_0\gamma} G_{r,3r}^{3r,0}\left[\delta_0\gamma \middle| \begin{matrix} \chi_1 \\ \chi_2 \end{matrix} \right] [1-\exp(-\tau_1\gamma)] \right. \\ & \left. + \tau_1 \exp(-\tau_1\gamma) G_{r+1,3r+1}^{3r,1}\left[\delta_0\gamma \middle| \begin{matrix} 1,\chi_1 \\ \chi_2,0 \end{matrix} \right] \right\} \Bigg) \\ & + \binom{K_2-1}{N_2-1} K_2 \sum_{j=0}^{K_2-N_2} \frac{\binom{K_2-N_2}{j}(-1)^j}{\tau_2} \Bigg(\tau_2 \exp(-\tau_1\gamma) \\ & - A \left\{ \frac{1}{\delta_0\gamma} \times [1-\exp(-\tau_2\gamma)] G_{r,3r}^{3r,0}\left[\delta_0\gamma \middle| \begin{matrix} \chi_1 \\ \chi_2 \end{matrix} \right] \right. \\ & \left. + \tau_2 \exp(-\tau_2\gamma) G_{r+1,3r+1}^{3r,1}\left[\delta_0\gamma \middle| \begin{matrix} 1,\chi_1 \\ \chi_2,0 \end{matrix} \right] \right\} \Bigg) \\ & - \binom{K_1-1}{N_1-1} K_1 \sum_{k=0}^{K_1-N_1} \frac{\binom{K_1-N_1}{k}}{\tau_1} \\ & \times (-1)^k \binom{K_2-1}{N_2-1} K_2 \sum_{j=0}^{K_2-N_2} \frac{\binom{K_2-N_2}{j}(-1)^j}{\tau_2} \\ & \times \Bigg(\tau_1 \exp(-\tau_1\gamma) + \tau_2 \exp(-\tau_2\gamma) - [\tau_1+\tau_2] \\ & \quad \exp(-[\tau_1+\tau_2]\gamma) - A \left\{ \frac{1}{\delta_0\gamma} \Big[1-\exp(-\tau_1\gamma) \right. \\ & \quad - \exp(-\tau_2\gamma) + \exp(-[\tau_1+\tau_2]\gamma) \Big] G_{r,3r}^{3r,0}\left[\delta_0\gamma \middle| \begin{matrix} \chi_1 \\ \chi_2 \end{matrix} \right] \\ & \quad + G_{r+1,3r+1}^{3r,1}\left[\delta_0\gamma \middle| \begin{matrix} 1,\chi_1 \\ \chi_2,0 \end{matrix} \right] \times \Big[\tau_1 \exp(-\tau_1\gamma) \\ & \quad \left. + \tau_2 \exp(-\tau_2\gamma) - \Big[\tau_1 + \tau_2 \Big] \exp(-[\tau_1+\tau_2]\gamma) \Big] \right\} \Bigg) \\ & + \frac{A}{\gamma} G_{r,3r}^{3r,0}\left[\delta_0\gamma \middle| \begin{matrix} \chi_1 \\ \chi_2 \end{matrix} \right]. \end{aligned} \tag{27}$$

Upon substituting (27) in (26) and using $\ln(1+\gamma) = G_{2,2}^{1,2}\left[\gamma \middle| \begin{matrix} 1,1 \\ 1,0 \end{matrix} \right]$ in integrals which include Meijer G-function, we get

$$\begin{aligned} C = & \frac{1}{\ln(2)} \Bigg\{ \binom{K_1-1}{N_1-1} K_1 \sum_{k=0}^{K_1-N_1} \frac{\binom{K_1-N_1}{k}(-1)^k}{\tau_1} \Bigg(\tau_1 \mathcal{I}_1 \\ & - A \left\{ \frac{1}{\delta_0} [\mathcal{I}_2 - \mathcal{I}_3] + \tau_1 \mathcal{I}_4 \right\} \Bigg) + \binom{K_2-1}{N_2-1} K_2 \\ & \times \sum_{j=0}^{K_2-N_2} \frac{\binom{K_2-N_2}{j}(-1)^j}{\tau_2} \left(\tau_2 \mathcal{I}_1' - A \left\{ \frac{1}{\delta_0} \left[\mathcal{I}_2 - \mathcal{I}_3' \right] + \tau_2 \mathcal{I}_4' \right\} \right) \\ & - K_1 \binom{K_1-1}{N_1-1} \sum_{k=0}^{K_1-N_1} \frac{\binom{K_1-N_1}{k}(-1)^k}{\tau_1} \times \binom{K_2-1}{N_2-1} K_2 \sum_{j=0}^{K_2-N_2} \\ & \times \frac{\binom{K_2-N_2}{j}(-1)^j}{\tau_2} \Bigg(\tau_1 \mathcal{I}_1 + \tau_2 \mathcal{I}_1' - [\tau_1+\tau_2] \mathcal{I}_5 \\ & - A \left\{ \frac{1}{\delta_0} \left[\mathcal{I}_2 - \mathcal{I}_3 - \mathcal{I}_3' \right] + \tau_1 \mathcal{I}_4 + \tau_2 \mathcal{I}_4' + \frac{1}{\delta_0} \mathcal{I}_6 \right. \\ & \left. - [\tau_1+\tau_2] \mathcal{I}_7 \right\} \Bigg) + \frac{1}{\delta_0} \mathcal{I}_2 \Bigg\}, \end{aligned} \tag{28}$$

where

$$\mathcal{I}_1 = \int_0^\infty \ln(1+\gamma) \exp(-\tau_1\gamma)\, d\gamma, \tag{29}$$

$$\mathcal{I}_2 = \int_0^\infty \gamma^{-1} G_{2,2}^{1,2}\left[\gamma \middle| \begin{matrix} 1,1 \\ 1,0 \end{matrix} \right] G_{r,3r}^{3r,0}\left[\delta_0\gamma \middle| \begin{matrix} \chi_1 \\ \chi_2 \end{matrix} \right] d\gamma, \tag{30}$$

$$\mathcal{I}_3 = \int_0^\infty \gamma^{-1} \exp(-\tau_1\gamma) G_{2,2}^{1,2}\left[\gamma \middle| \begin{matrix} 1,1 \\ 1,0 \end{matrix} \right] G_{r,3r}^{3r,0}\left[\delta_0\gamma \middle| \begin{matrix} \chi_1 \\ \chi_2 \end{matrix} \right] d\gamma, \tag{31}$$

$$\mathcal{I}_4 = \int_0^\infty \exp(-\tau_1\gamma) G_{2,2}^{1,2}\left[\gamma \middle| \begin{matrix} 1,1 \\ 1,0 \end{matrix} \right] G_{r+1,3r+1}^{3r,1}\left[\delta_0\gamma \middle| \begin{matrix} 1,\chi_1 \\ \chi_2,0 \end{matrix} \right] d\gamma, \tag{32}$$

$$\mathcal{I}_5 = \int_0^\infty \ln(1+\gamma) \exp(-[\tau_1+\tau_2]\gamma)\, d\gamma, \tag{33}$$

$$\begin{aligned} \mathcal{I}_6 = & \int_0^\infty \gamma^{-1} \exp(-[\tau_1+\tau_2]\gamma) G_{2,2}^{1,2}\left[\gamma \middle| \begin{matrix} 1,1 \\ 1,0 \end{matrix} \right] \\ & \times G_{r,3r}^{3r,0}\left[\delta_0\gamma \middle| \begin{matrix} \chi_1 \\ \chi_2 \end{matrix} \right] d\gamma, \end{aligned} \tag{34}$$

$$\begin{aligned} \mathcal{I}_7 = & \int_0^\infty \exp(-[\tau_1+\tau_2]\gamma) G_{2,2}^{1,2}\left[\begin{matrix} \gamma \\ 1,0 \end{matrix} \middle| 1,1 \right] \\ & \times G_{r+1,3r+1}^{3r,1}\left[\delta_0\gamma \middle| \begin{matrix} 1,\chi_1 \\ \chi_2,0 \end{matrix} \right] d\gamma, \end{aligned} \tag{35}$$

where $\mathcal{I}_1' = \mathcal{I}_1$, $\mathcal{I}_3' = \mathcal{I}_3$, and $\mathcal{I}_4' = \mathcal{I}_4$ with replacing k by j, N_1 by N_2, and λ_{u,r_1} by $\lambda_{r_2,u}$, respectively.

The integrals $\mathcal{I}_1$ and $\mathcal{I}_1^{'}$ can be obtained using Eq. 4.337.2 in [32], and the other integrals can be obtained with the help of the integral properties of Meijer G-function ([36, Eq. 07.34.21.0011.01] and [36, Eq. 07.34.21.0081.01]). Upon doing these integrations, we get the following:

$$
\begin{aligned}
C = \frac{1}{\ln(2)} \Bigg\{ & \binom{K_1-1}{N_1-1} K_1 \sum_{k=0}^{K_1-N_1} \frac{\binom{K_1-N_1}{k}(-1)^k}{\tau_1} \Bigg(-\exp(\tau_1)\,\mathrm{E_i}(-\tau_1) \\
& - A \Bigg\{ \frac{1}{\delta_0} \Bigg[\mathrm{G}^{3r+2,1}_{r+2,3r+2} \left[\delta_0 \,\middle|\, \begin{matrix} 0,1,\chi_1 \\ \chi_2,0 \end{matrix} \right] - \mathrm{G}^{0,1:1,2:3r,0}_{1,0:2,2:r,3r} \\
& \times \left[\tfrac{1}{\tau_1}, \delta_0\tau_1 \,\middle|\, \begin{matrix} 1 \\ - \end{matrix} \,\middle|\, \begin{matrix} 1,1 \\ 1,0 \end{matrix} \,\middle|\, \begin{matrix} \chi_1 \\ \chi_2 \end{matrix} \right] \Bigg] \mathrm{G}^{0,1:1,2:3r,1}_{1,0:2,2:r+1,3r+1} \\
& \times \left[\tfrac{1}{\tau_1}, \delta_0\tau_1 \,\middle|\, \begin{matrix} 2 \\ - \end{matrix} \,\middle|\, \begin{matrix} 1,1 \\ 1,0 \end{matrix} \,\middle|\, \begin{matrix} 1,\chi_1 \\ \chi_2,0 \end{matrix} \right] \times (\tau_1)^2 \Bigg\} \Bigg) + \binom{K_2-1}{N_2-1} K_2 \\
& \times \sum_{j=0}^{K_2-N_2} \binom{K_2-N_2}{j} (-1)^j (\tau_2)^{-1} \Bigg(-\exp(\tau_2)\,\mathrm{E_i}(-\tau_2) \\
& - A \Bigg\{ \frac{1}{\delta_0} \Bigg[\mathrm{G}^{3r+2,1}_{r+2,3r+2} \left[\delta_0 \,\middle|\, \begin{matrix} 0,1,\chi_1 \\ \chi_2,0 \end{matrix} \right] - \mathrm{G}^{0,1:1,2:3r,0}_{1,0:2,2:r,3r} \\
& \times \left[\tfrac{1}{\tau_2}, \delta_0\tau_2 \,\middle|\, \begin{matrix} 1 \\ - \end{matrix} \,\middle|\, \begin{matrix} 1,1 \\ 1,0 \end{matrix} \,\middle|\, \begin{matrix} \chi_1 \\ \chi_2 \end{matrix} \right] \Bigg] + (\tau_2)^2 \mathrm{G}^{0,1:1,2:3r,1}_{1,0:2,2:r+1,3r+1} \\
& \times \left[\tfrac{1}{\tau_2}, \delta_0\tau_2 \,\middle|\, \begin{matrix} 2 \\ - \end{matrix} \,\middle|\, \begin{matrix} 1,1 \\ 1,0 \end{matrix} \,\middle|\, \begin{matrix} 1,\chi_1 \\ \chi_2,0 \end{matrix} \right] \Bigg\} \Bigg) - \binom{K_1-1}{N_1-1} K_1 \\
& \times \sum_{k=0}^{K_1-N_1} \frac{\binom{K_1-N_1}{k}(-1)^k}{\tau_1} \binom{K_2-1}{N_2-1} K_2 \sum_{j=0}^{K_2-N_2} (-1)^j \frac{\binom{K_2-N_2}{j}}{\tau_2} \\
& \times \Bigg(-\exp(\tau_1)\,\mathrm{E_i}(-\tau_1) - \exp(\tau_2)\,\mathrm{E_i}(-\tau_2) + \exp(\tau_1+\tau_2) \\
& \times \mathrm{E_i}(-(\tau_1+\tau_2)) - A \Bigg\{ \frac{1}{\delta_0} \Bigg[\mathrm{G}^{3r+2,1}_{r+2,3r+2} \left[\delta_0 \,\middle|\, \begin{matrix} 0,1,\chi_1 \\ \chi_2,0 \end{matrix} \right] - \mathrm{G}^{0,1:1,2:3r,0}_{1,0:2,2:r,3r} \\
& \times \left[\tfrac{1}{\tau_1}, \delta_0\tau_1 \,\middle|\, \begin{matrix} 1 \\ - \end{matrix} \,\middle|\, \begin{matrix} 1,1 \\ 1,0 \end{matrix} \,\middle|\, \begin{matrix} \chi_1 \\ \chi_2 \end{matrix} \right] - \mathrm{G}^{0,1:1,2:3r,0}_{1,0:2,2:r,3r} \left[\tfrac{1}{\tau_2}, \delta_0\tau_2 \,\middle|\, \begin{matrix} 1 \\ - \end{matrix} \,\middle|\, \begin{matrix} 1,1 \\ 1,0 \end{matrix} \,\middle|\, \begin{matrix} \chi_1 \\ \chi_2 \end{matrix} \right] \\
& + \mathrm{G}^{0,1:1,2:3r,0}_{1,0:2,2:r,3r} \left[\tfrac{1}{[\tau_1+\tau_2]}, \delta_0\,[\tau_1+\tau_2] \,\middle|\, \begin{matrix} 1 \\ - \end{matrix} \,\middle|\, \begin{matrix} 1,1 \\ 1,0 \end{matrix} \,\middle|\, \begin{matrix} \chi_1 \\ \chi_2 \end{matrix} \right] \Bigg] + (\tau_1)^2 \\
& \times \mathrm{G}^{0,1:1,2:3r,1}_{1,0:2,2:r+1,3r+1} \left[\tfrac{1}{\tau_1}, \delta_0\tau_1 \,\middle|\, \begin{matrix} 2 \\ - \end{matrix} \,\middle|\, \begin{matrix} 1,1 \\ 1,0 \end{matrix} \,\middle|\, \begin{matrix} 1,\chi_1 \\ \chi_2,0 \end{matrix} \right] \\
& + (\tau_2)^2 \mathrm{G}^{0,1:1,2:3r,1}_{1,0:2,2:r+1,3r+1} \left[\tfrac{1}{\tau_2}, \delta_0\tau_2 \,\middle|\, \begin{matrix} 2 \\ - \end{matrix} \,\middle|\, \begin{matrix} 1,1 \\ 1,0 \end{matrix} \,\middle|\, \begin{matrix} 1,\chi_1 \\ \chi_2,0 \end{matrix} \right] - [\tau_1+\tau_2]^2 \\
& \times \mathrm{G}^{0,1:1,2:3r,0}_{1,0:2,2:r,3r} \left[\tfrac{1}{[\tau_1+\tau_2]}, \delta_0[\,\tau_1+\tau_2] \,\middle|\, \begin{matrix} 1 \\ - \end{matrix} \,\middle|\, \begin{matrix} 1,1 \\ 1,0 \end{matrix} \,\middle|\, \begin{matrix} \chi_1 \\ \chi_2 \end{matrix} \right] \Bigg\} \\
& + \frac{1}{\delta_0} \mathrm{G}^{3r+2,1}_{r+2,3r+2} \left[\delta_0 \,\middle|\, \begin{matrix} 0,1,\chi_1 \\ \chi_2,0 \end{matrix} \right] \Bigg\},
\end{aligned}
\tag{36}
$$

where $\mathrm{E_i}(.)$ is the exponential integral function defined by Eq. 8.211.1 in [32], and $G\,[Z_1, Z_2|.|.|.]$ is the extended generalized bivariate Meijer G-function. Note that in order to evaluate the expression in (36), a Mathematica code similar to the one provided in Table 2 in [41] has been used here.

4 Asymptotic outage performance and power allocation

Due to complexity of the achieved expressions in the previous section, it is hard to easily study the effect of various system parameters and get more insights about the system performance. Therefore, we see that it is important to derive simple expressions for the outage probability which will be helpful in achieving more insights about the system behavior. These expressions will be used also in allocating the transmission power for the transmitting nodes of the system (first hop source's power, second hop relay's power, and third hop relay's power).

4.1 Asymptotic outage probability

The outage probability can be written at the high SNR regime as $P_{\mathrm{out}} \simeq (G_{\mathrm{c}}\mathrm{SNR})^{-G_{\mathrm{d}}}$, where G_{c} and G_{d} are the coding gain and diversity order of the system, respectively [42]. Obviously, G_{c} represents the horizontal shift in the outage probability performance relative to the benchmark curve $(\mathrm{SNR})^{-G_{\mathrm{d}}}$ and G_{d} refers to the increase in the slope of the outage probability vs SNR curve. Therefore, the parameters on which the diversity order depends will affect the slope of the outage probability curves and the parameters on which the coding gain depends will affect the position of the curves. Obtaining the outage probability in this simple form allows us to easily study and know the effect of each system parameter on the system performance instead of dealing with the long/complex expressions derived in Section 3. Notice that such an accurate approximation has been widely used in the conventional cooperative diversity systems.

Here, we consider the case of identical sources' channels ($\lambda_{1,\mathrm{r}_1} = \lambda_{2,\mathrm{r}_1} = \cdots = \lambda_{K_1,\mathrm{r}_1} = \lambda_{u,\mathrm{r}_1}$) and identical destinations' channels ($\lambda_{\mathrm{r}_2,1} = \lambda_{\mathrm{r}_2,2} = \cdots = \lambda_{\mathrm{r}_2,K_2} = \lambda_{\mathrm{r}_2,u}$). Again, we follow the same procedure that we followed before in Section 3 in obtaining the outage probability of the proposed scenario by dealing with the approximate CDF of each hop separately and then calculating the approximate CDF of the e2e SNR.

4.1.1 First hop link

Upon using the Taylor series representation of the exponential term in the CDF $F_{\gamma_{\mathrm{U,R_1}}}(\gamma) = 1 - \exp\left(-\lambda_{u,\mathrm{r}_1}\gamma\right)$, we get $F_{\gamma_{\mathrm{U,R_1}}}(\gamma) \approx 1 - \big[1 - (\lambda_{u,\mathrm{r}_1}\gamma) + \frac{(\lambda_{u,\mathrm{r}_1}\gamma)^2}{2!} -$

$\frac{(\lambda_{u,\mathrm{r}_1}\gamma)^3}{3!} + \frac{(\lambda_{u,\mathrm{r}_1}\gamma)^4}{4!} - \cdots]$, which for high values of $\bar{\gamma}_{u,\mathrm{r}_1}$ ($\bar{\gamma}_{u,\mathrm{r}_1} \to \infty$) simplifies to $\lambda_{u,\mathrm{r}_1}\gamma$ and hence, the PDF $f_{\gamma_{\mathrm{U,R}_1}}(\gamma)$ simplifies to λ_{u,r_1}. Upon substituting these statistics in (18) and integrating the result using $\int_0^\gamma f_{\gamma_{\mathrm{U_{Sel},R_1}}}(t)dt$, we get

$$F_{\gamma_{\mathrm{U_{Sel},R_1}}}(\gamma) \simeq \binom{K_1-1}{N_1-1} K_1 (\lambda_{u,\mathrm{r}_1})^{K_1-N_1+1} \times \sum_{k=0}^{N_1-1} \frac{\binom{N_1-1}{k}(-1)^k(\lambda_{u,\mathrm{r}_1})^k}{(k+K_1-N_1+1)} \gamma^{k+K_1-N_1+1}. \tag{37}$$

The CDF in (37) is still dominant for the first term of the summation and hence, it can be further simplified to

$$F_{\gamma_{\mathrm{U_{Sel},R_1}}}(\gamma) \simeq \binom{K_1-1}{N_1-1} K_1 (\lambda_{u,\mathrm{r}_1})^{K_1-N_1+1} \frac{\gamma^{K_1-N_1+1}}{(K_1-N_1+1)}. \tag{38}$$

4.1.2 Second hop link

From Eq. 07.34.06.006.01 in [36], as $\bar{\gamma}_{\mathrm{r}_1,\mathrm{r}_2} \to \infty$ or, equivalently, as $z \to 0$, the Meijer G-function can be approximated using the following series representation:

$$\mathrm{G}_{p,q}^{m,n}\left[z \middle| \begin{matrix} a_1,\ldots,a_p \\ b_1,\ldots,b_q \end{matrix} \right] = \sum_{k=1}^{m} \frac{\prod_{j=1,j\neq k}^{m} \Gamma(b_j-b_k) \prod_{j=1}^{n} \Gamma(1-a_j+b_k)}{\prod_{j=n+1}^{p} \Gamma(a_j-b_k) \prod_{j=m+1}^{q} \Gamma(1-b_j+b_k)} z^{b_k}(1+o(z)), \tag{39}$$

where $p \leq q$ is required. Here, we use the same approach that was used in [43] in writing the outage probability for this case. Defining $\nu = \min\{\zeta^2,\alpha,\beta\}$, then we have

$$F_{\gamma_{\mathrm{R_1,R_2}}}(\gamma) \simeq \Upsilon \left(\frac{\gamma}{\bar{\gamma}_{\mathrm{r}_1,\mathrm{r}_2}} \right)^{\frac{\nu}{r}}, \tag{40}$$

where Υ is constant. In order to find the value of Υ, we first rewrite the CDF $F_{\gamma_{\mathrm{R_1,R_2}}}(\gamma)$ provided in (20) using the asymptotic expression of the Meijer provided in (39). By matching the Meijer function with its asymptotic representation, we find that $m=3r, n=1, p=r+1, q=3r+1$. Now, the asymptotic CDF $F_{\gamma_{\mathrm{R_1,R_2}}}(\gamma)$ can be written with ignoring the high order terms as

$$F_{\gamma_{\mathrm{R_1,R_2}}}(\gamma) = A \sum_{k=1}^{3r} \frac{\prod_{j=1,j\neq k}^{3r} \Gamma(b_j-b_k)\Gamma(1-a_1+b_k)}{\prod_{j=2}^{r+1} \Gamma(a_j-b_k)\Gamma(1-b_{3r+1}+b_k)} \times B^{b_k/r} \left(\frac{\gamma}{\bar{\gamma}_{\mathrm{r}_1,\mathrm{r}_2}} \right)^{\frac{b_k}{r}}, \tag{41}$$

where $b_j = \chi_2(j)$, $j=1,\ldots,3r$, $b_{3r+1}=0$, $b_k = \min\{\zeta^2,\alpha,\beta\}$, $a_j=\chi_1(j)$, for $j=1,\ldots,r+1$, $a_1=1$, and $b_{3r+1}=0$. For the case of IM/DD receiver ($r=2$), (41) simplifies to

$$F_{\gamma_{\mathrm{R_1,R_2}}}(\gamma) = A \sum_{k=1}^{6} \frac{\prod_{j=1,j\neq k}^{6} \Gamma(b_j-b_k)\Gamma(b_k)}{\prod_{j=2}^{3} \Gamma(a_j-b_k)\Gamma(1+b_k)} \times B^{b_k/2} \left(\frac{\gamma}{\bar{\gamma}_{\mathrm{r}_1,\mathrm{r}_2}} \right)^{\frac{b_k}{2}}, \tag{42}$$

where $b_j = \chi_2(j)$, $j=1,\ldots,6$, $b_7=0$, $a_j=\chi_1(j)$, for $j=1,\ldots,3$, $a_1=1$, and $b_7=0$. Comparing (42) with the second term of (40) shows that the constant Υ equals

$$\Upsilon = A \sum_{k=1}^{6} \frac{\prod_{j=1,j\neq k}^{6} \Gamma(b_j-b_k)\Gamma(b_k)}{\prod_{j=2}^{3} \Gamma(a_j-b_k)\Gamma(1+b_k)} B^{b_k/2}, \tag{43}$$

where $b_k = \nu$.

4.1.3 Third hop link

Similar to first hop link analysis, as $\bar{\gamma}_{\mathrm{r}_2,u} \to \infty$, the CDF and PDF of the third hop SNR $F_{\gamma_{\mathrm{R_2,D}}}(\gamma)$ and $f_{\gamma_{\mathrm{R_2,D}}}(\gamma)$ simplify to $\lambda_{\mathrm{r}_2,u}\gamma$ and $\lambda_{\mathrm{r}_2,u}$, respectively. Upon substituting these statistics in (18) and integrating the result using $\int_0^\gamma f_{\gamma_{\mathrm{R_2,D_{Sel}}}}(t)dt$, we get

$$F_{\gamma_{\mathrm{R_2,D_{Sel}}}}(\gamma) \simeq \binom{K_2-1}{N_2-1} K_2 (\lambda_{\mathrm{r}_2,u})^{K_2-N_2+1} \times \sum_{j=0}^{N_2-1} \frac{\binom{N_2-1}{j}(-1)^j(\lambda_{\mathrm{r}_2,u})^j}{(j+K_2-N_2+1)} \gamma^{j+K_2-N_2+1}. \tag{44}$$

The CDF in (44) is still dominant for the first term of the summation and hence, it can be further simplified to

$$F_{\gamma_{\mathrm{R_2,D_{Sel}}}}(\gamma) \simeq \binom{K_2-1}{N_2-1} K_2 (\lambda_{\mathrm{r}_2,u})^{K_2-N_2+1} \frac{\gamma^{K_2-N_2+1}}{(K_2-N_2+1)}. \tag{45}$$

With the aim of obtaining the diversity order and coding gain of the system, the CDF in (16) can be simplified at high SNR values to be

$$F_{\gamma_{\mathrm{D}}}(\gamma) \simeq F_{\gamma_{\mathrm{U_{Sel},R_1}}}(\gamma) + F_{\gamma_{\mathrm{R_1,R_2}}}(\gamma) + F_{\gamma_{\mathrm{R_2,D_{Sel}}}}(\gamma), \tag{46}$$

where the remaining terms in (16) are omitted and this is accurate for high SNRs.

Substituting (38), (39), and (45) in (46), the outage probability can be written at high SNR values as

$$P_{\text{out}}^{\infty} = \binom{K_1-1}{N_1-1} K_1 (\bar{\gamma}_{u,\text{r}_1})^{-(K_1-N_1+1)} \frac{(\gamma_{\text{out}})^{K_1-N_1+1}}{(K_1-N_1+1)} + \left(\frac{\Upsilon^{-\frac{r}{\nu}}}{\gamma_{\text{out}}}\bar{\gamma}_{\text{r}_1,\text{r}_2}\right)^{-\frac{\nu}{r}} + \binom{K_2-1}{N_2-1} K_2 (\bar{\gamma}_{\text{r}_2,u})^{-(K_2-N_2+1)} \times \frac{(\gamma_{\text{out}})^{K_2-N_2+1}}{(K_2-N_2+1)}. \tag{47}$$

It is clear from (47) that the performance of the considered relay network will be dominated by the worst link among the available three links, the first RF link, the FSO link, and the third RF link. This domination depends on the parameters of these links. Therefore, the diversity order (G_{d}) of the triple-hop mixed RF/FSO/RF relay network with generalized order user scheduling is equal to $\min(K_1-N_1+1, \nu/r, K_2-N_2+1)$ and based on the value of the diversity order, one of the following three cases could represent the overall system performance:

Case 1 (One hop is dominant)**.** In this case, the coding gain (G_{c}) can be written as

$$G_{\text{c}} = \begin{cases} \left[\binom{K_1-1}{N_1-1} K_1 \frac{(\gamma_{\text{out}})^{K_1-N_1+1}}{(K_1-N_1+1)}\right]^{-\frac{1}{K_1-N_1+1}}, & G_{\text{d}} = K_1-N_1+1, \\ \frac{\Upsilon^{-\frac{r}{\nu}}}{\gamma_{\text{out}}}, & G_{\text{d}} = \frac{\nu}{r}, \\ \left[\binom{K_2-1}{N_2-1} K_2 \frac{(\gamma_{\text{out}})^{K_2-N_2+1}}{(K_2-N_2+1)}\right]^{-\frac{1}{K_2-N_2+1}}, & G_{\text{d}} = K_2-N_2+1. \end{cases} \tag{48}$$

Case 2 (Two hops are dominant)**.** In this case, the coding gain can be written as

$$G_{\text{c}} = \begin{cases} \frac{1}{2}\left\{ \left[\binom{K_1-1}{N_1-1} K_1 \frac{(\gamma_{\text{out}})^{K_1-N_1+1}}{(K_1-N_1+1)}\right]^{-\frac{1}{K_1-N_1+1}} + \left[\binom{K_2-1}{N_2-1} K_2 \frac{(\gamma_{\text{out}})^{K_2-N_2+1}}{(K_2-N_2+1)}\right]^{-\frac{1}{K_2-N_2+1}} \right\}, & G_{\text{d}} = K_1-N_1+1 = K_2-N_2+1, \\ \frac{1}{2}\left\{ \left[\binom{K_1-1}{N_1-1} K_1 \frac{(\gamma_{\text{out}})^{K_1-N_1+1}}{(K_1-N_1+1)}\right]^{-\frac{1}{K_1-N_1+1}} + \frac{\Upsilon^{-\frac{r}{\nu}}}{\gamma_{\text{out}}} \right\}, & G_{\text{d}} = K_1-N_1+1 = \frac{\nu}{r}, \\ \frac{1}{2}\left\{ \left[\binom{K_2-1}{N_2-1} K_2 \frac{(\gamma_{\text{out}})^{K_2-N_2+1}}{(K_2-N_2+1)}\right]^{-\frac{1}{K_2-N_2+1}} + \frac{\Upsilon^{-\frac{r}{\nu}}}{\gamma_{\text{out}}} \right\}, & G_{\text{d}} = K_2-N_2+1 = \frac{\nu}{r}. \end{cases} \tag{49}$$

Case 3 (Three hops have the same diversity order)**.** In this case, the coding gain can be written as

$$G_{\text{c}} = \begin{cases} \frac{1}{3}\left\{ \left[\binom{K_1-1}{N_1-1} K_1 \frac{(\gamma_{\text{out}})^{K_1-N_1+1}}{(K_1-N_1+1)}\right]^{-\frac{1}{K_1-N_1+1}} + \frac{\Upsilon^{-\frac{r}{\nu}}}{\gamma_{\text{sout}}} + \left[\binom{K_2-1}{N_2-1} K_2 \frac{(\gamma_{\text{out}})^{K_2-N_2+1}}{-(K_2-N_2+1)}\right]^{-\frac{1}{K_2-N_2+1}} \right\}, & G_{\text{d}} = K_1-N_1+1 = K_2-N_2+1 = \frac{\nu}{r}. \end{cases} \tag{50}$$

In summary, the system performance could be dominated by the following: (1) the first hop link (i.e., K_1 and N_1) when it is the worst link among the three links; (2) the second hop link (i.e., ζ^2, α, and β) when it is the worst link among the three links; and (3) the third hop link (i.e., K_2 and N_2) when it is the worst link among the three links. It is very important to mention here that if the diversity orders of two hops are equal and they are the minimum compared to that of the third hop, the coding gain of the system in this case equals the summation of the coding gains of the two hops which dominate the system performance divided by 2. Similarly, if the diversity orders of the three hops are equal, the coding gain of the system in this case equals the summation of the coding gains of the three hops divided by 3.

4.2 Power allocation

In this section, we aim to derive the optimum adaptive power allocation for the transmitting nodes in the system. In the proposed power allocation protocol, the powers of all transmitting nodes (selected source, first relay, and second relay) in the system are considered to be variables. Assuming that we may have two different cases in regard to the transmission power of the first relay: the allocated power for the first relay is less than the peak/maximum allowed power and in this case, the power allocation protocol is optimum and the second case where the allocated power for the first relay is larger than the peak power and here the extra allocated power will be saved.

We denote the distance between the first hop K_1 sources and relay R_1 by d_{s,r_1}, the distance between the relays R_1 and R_2 by $d_{\text{r}_1,\text{r}_2}$, while the distance between the relay R_2 and third hop K_2 destinations by $d_{\text{r}_2,\text{d}}$. We consider a total distance of D_{tot} between the first hop sources and third hop destinations. The total distance D_{tot} can be written as $D_{\text{tot}} = d_{\text{s},\text{r}_1} + d_{\text{r}_1,\text{r}_2} + d_{\text{r}_2,\text{d}}$. Under the scenario where the received power decays with the distance, we can express the average value of SNR in the hop between the K_1 sources and relay R_1 as $\bar{\gamma}_{\mathsf{s,r}_1} = P_{\mathsf{s,r}_1} d_{\mathsf{s,r}_1}^{-\mu}$, where $P_{\mathsf{s,r}_1} = \frac{P_{u,\mathsf{r}_1}}{K_1} = \frac{E_{\mathsf{s,r}_1}}{N_0}$, μ is the path loss exponent and is equal for all hops to a value greater than 1, and N_0 is AWGN power which is assumed equal for the three hops. Similarly, we can express the average value of SNR in the second hop as $\bar{\gamma}_{\mathsf{r}_1,\mathsf{r}_2} = P_{\mathsf{r}_1,\mathsf{r}_2} d_{\mathsf{r}_1,\mathsf{r}_2}^{-\mu}$, where $P_{\mathsf{r}_1,\mathsf{r}_2} = \frac{E_{\mathsf{r}_1,\mathsf{r}_2}}{N_0}$. The average value of SNR in the hop between the relay R_2 and K_2 destinations can be expressed as $\bar{\gamma}_{\mathsf{r}_2,\mathsf{d}} = P_{\mathsf{r}_2,\mathsf{d}} d_{\mathsf{r}_2,\mathsf{d}}^{-\mu}$, where $P_{\mathsf{r}_2,\mathsf{d}} = \frac{P_{\mathsf{r}_2,\mathsf{d}}}{K_1} = \frac{E_{\mathsf{r}_2,\mathsf{d}}}{N_0}$. Finally, the power constraint can be written as $P_{\text{tot}} = P_{\mathsf{s,r}_1} + P_{\mathsf{r}_1,\mathsf{r}_2} + P_{\mathsf{r}_2,\mathsf{d}}$.

We derive the optimal power allocation that minimizes the outage probability subject to sum power constraint as below

$$\left(P^*_{\mathsf{s,r}_1}, P^*_{\mathsf{r}_1,\mathsf{r}_2}, P^*_{\mathsf{r}_2,\mathsf{d}}\right) = \arg \min_{(P_{\mathsf{s,r}_1}, P_{\mathsf{r}_1,\mathsf{r}_2}, P_{\mathsf{r}_2,\mathsf{d}})} F_{\gamma_\mathsf{D}}(\gamma_{\text{out}}), \quad (51)$$

subject to $P_{\text{tot}} = P_{\mathsf{s,r}_1} + P_{\mathsf{r}_1,\mathsf{r}_2} + P_{\mathsf{r}_2,\mathsf{d}}$.

The asymptotic expression for $F_{\gamma_\mathsf{D}}(\gamma_{\text{out}})$ can be rewritten as follows

$$\begin{aligned} F_{\gamma_\mathsf{D}}(\gamma_{\text{out}}) \simeq & \binom{K_1-1}{N_1-1} K_1 \left(\frac{d^\mu_{\mathsf{s,r}_1}}{P_{\mathsf{s,r}_1}}\right)^{K_1-N_1+1} \frac{(\gamma_{\text{out}})^{K_1-N_1+1}}{(K_1-N_1+1)} \\ & + \frac{\gamma_{\text{out}} A B d^\mu_{\mathsf{r}_1,\mathsf{r}_2}}{P_{\mathsf{r}_1,\mathsf{r}_2}} + \binom{K_2-1}{N_2-1} K_2 \\ & \times \left(\frac{d^\mu_{\mathsf{r}_2,\mathsf{d}}}{P_{\mathsf{r}_2,\mathsf{d}}}\right)^{K_2-N_2+1} \frac{(\gamma_{\text{out}})^{K_2-N_2+1}}{(K_2-N_2+1)}. \end{aligned} \quad (52)$$

To simplify the understanding of the next steps of optimization, we introduce here the Lagrangian multipliers method which is used in deriving of the optimal transmission powers of the transmitting nodes of the system. This method is a very common strategy used for finding the local maxima and minima of a function subject to equality constraints. The method depends on defining a Lagrange multiplier, Lagrange function, and a constraint. The Lagrange function is then defined as a summation of the constraint multiplied by the Lagrange multiplier and the original constrained problem or function. Note that the original constrained function and constraint are functions of the unknowns which we need to find their optimum values. Then, the Lagrange function is differentiated with respect to each unknown and equated by zero trying to find a solution to that unknown in terms of the Lagrange multiplier. Then, the unknowns are written again (in terms of the Lagrange multiplier) to formulate the constraint. After that, the constraint is solved in order to obtain the Lagrange multiplier. Finally, the obtained Lagrange multiplier is used in finding the optimal values of the unknowns.

Now, using the Lagrangian multipliers method for our problem, we define the Lagrange function as

$$\begin{aligned} \mathcal{F}(P_{\mathsf{s,r}_1}, P_{\mathsf{r}_1,\mathsf{r}_2}, P_{\mathsf{r}_2,\mathsf{d}}, \lambda) = & F_{\gamma_\mathsf{D}}(P_{\mathsf{s,r}_1}, P_{\mathsf{r}_1,\mathsf{r}_2}, P_{\mathsf{r}_2,\mathsf{d}}) \\ & + \lambda g(P_{\mathsf{s,r}_1}, P_{\mathsf{r}_1,\mathsf{r}_2}, P_{\mathsf{r}_2,\mathsf{d}}), \end{aligned} \quad (53)$$

where λ is the Lagrange multiplier and $g(.)$ is the power constraint. The function in (53) can be rewritten as

$$\begin{aligned} \mathcal{F}(P_{\mathsf{s,r}_1}, P_{\mathsf{r}_1,\mathsf{r}_2}, P_{\mathsf{r}_2,\mathsf{d}}, \lambda) = & \binom{K_1-1}{N_1-1} K_1 \left(\frac{d^\mu_{\mathsf{s,r}_1}}{P_{\mathsf{s,r}_1}}\right)^{K_1-N_1+1} \\ & \times \frac{(\gamma_{\text{out}})^{K_1-N_1+1}}{(K_1-N_1+1)} + \frac{\gamma_{\text{out}} A B d^\mu_{\mathsf{r}_1,\mathsf{r}_2}}{P_{\mathsf{r}_1,\mathsf{r}_2}} \\ & + \binom{K_2-1}{N_2-1} \times K_2 \left(\frac{d^\mu_{\mathsf{r}_2,\mathsf{d}}}{P_{\mathsf{r}_2,\mathsf{d}}}\right)^{K_2-N_2+1} \\ & \times \frac{(\gamma_{\text{out}})^{K_2-N_2+1}}{(K_2-N_2+1)} + \lambda (P_{\mathsf{s,r}_1} \\ & + P_{\mathsf{r}_1,\mathsf{r}_2} + P_{\mathsf{r}_2,\mathsf{d}} - P_{\text{tot}}). \end{aligned} \quad (54)$$

Taking the first derivative with respect to $P_{\mathsf{s,r}_1}$ and equate it by zero, we get

$$\begin{aligned} \frac{\partial \mathcal{F}}{\partial P_{\mathsf{s,r}_1}} = & -\binom{K_1-1}{N_1-1} K_1 \left(d^\mu_{\mathsf{s,r}_1} \gamma_{\text{out}}\right)^{K_1-N_1+1} \\ & \times \left(P^*_{\mathsf{s,r}_1}\right)^{-(K_1-N_1+2)} + \lambda = 0. \end{aligned} \quad (55)$$

Solving for $P^*_{\mathsf{s,r}_1}$, we get

$$P^*_{\mathsf{s,r}_1} = \left[\binom{K_1-1}{N_1-1} K_1\right]^{K_1-N_1+3} d^\mu_{\mathsf{s,r}_1} \gamma_{\text{out}} \lambda^{\frac{-1}{(K_1-N_1+2)}}. \quad (56)$$

Similarly, differentiating $\mathcal{F}$ with respect to $P_{\mathsf{r}_1,\mathsf{r}_2}$ and equating the result by zero and solving for $P_{\mathsf{r}_1,\mathsf{r}_2}$, we get

$$P^*_{\mathsf{r}_1,\mathsf{r}_2} = \left[A B d^\mu_{\mathsf{r}_1,\mathsf{r}_2} \gamma_{\text{out}}\right]^{\frac{1}{2}} \lambda^{\frac{-1}{2}}. \quad (57)$$

Following the same method of the first hop with the third hop, we get

$$P^*_{\mathsf{r}_2,\mathsf{d}} = \left[\binom{K_2-1}{N_2-1} K_2\right]^{K_2-N_2+3} d^\mu_{\mathsf{r}_2,\mathsf{d}} \gamma_{\text{out}} \lambda^{\frac{-1}{(K_2-N_2+2)}}. \quad (58)$$

Now, summing the three individual powers' results in the total power as

$$\begin{aligned} & \left[\binom{K_1-1}{N_1-1} K_1\right]^{K_1-N_1+3} d^\mu_{\mathsf{s,r}_1} \gamma_{\text{out}} \lambda^{\frac{-1}{(K_1-N_1+2)}} \\ & + \left[A B d^\mu_{\mathsf{r}_1,\mathsf{r}_2} \gamma_{\text{out}}\right]^{\frac{1}{2}} \lambda^{\frac{-1}{2}} + \left[\binom{K_2-1}{N_2-1} K_2\right]^{K_2-N_2+3} d^\mu_{\mathsf{r}_2,\mathsf{d}} \\ & \times \gamma_{\text{out}} \lambda^{\frac{-1}{(K_2-N_2+2)}} = P_{\text{tot}}. \end{aligned} \quad (59)$$

It is clear from (59) that finding a closed-form expression for λ would be very difficult. However, a numerical solution can be found by standard iterative root-finding algorithms, such as the Bisection's method and Newton's method. It is worthwhile to mention that the closed-form expressions for some special cases can be found such as the case where $K_1 = K_2 = 1$ and $N_1 = N_2 = 1$. For this case, (59) reduces to

$$d^{\mu}_{\mathrm{s,r_1}}\gamma_{\mathrm{out}}\lambda^{\frac{-1}{2}} + \left[ABd^{\mu}_{\mathrm{r_1,r_2}}\gamma_{\mathrm{out}}\right]^{\frac{1}{2}}\lambda^{\frac{-1}{2}} + d^{\mu}_{\mathrm{r_2,d}}\lambda^{\frac{-1}{2}} = P_{\mathrm{tot}}. \tag{60}$$

Solving for λ gives

$$\lambda = \left\{\frac{P_{\mathrm{tot}}}{\gamma_{\mathrm{out}}(d^{\mu}_{\mathrm{s,r_1}} + d^{\mu}_{\mathrm{r_2,d}}) + \left[ABd^{\mu}_{\mathrm{r_1,r_2}}\gamma_{\mathrm{out}}\right]^{\frac{1}{2}}}\right\}^{-2}. \tag{61}$$

Upon substituting (61) in (56), (57), and (58), we get the optimum transmission powers as

$$P^{*}_{\mathrm{s,r_1}} = \frac{d^{\mu}_{\mathrm{s,r_1}}\gamma_{\mathrm{out}}P_{\mathrm{tot}}}{\gamma_{\mathrm{out}}(d^{\mu}_{\mathrm{s,r_1}} + d^{\mu}_{\mathrm{r_2,d}}) + \left[ABd^{\mu}_{\mathrm{r_1,r_2}}\gamma_{\mathrm{out}}\right]^{\frac{1}{2}}}, \tag{62}$$

$$P^{*}_{\mathrm{r_1,r_2}} = \frac{\left[ABd^{\mu}_{\mathrm{r_1,r_2}}\gamma_{\mathrm{out}}\right]^{\frac{1}{2}}P_{\mathrm{tot}}}{\gamma_{\mathrm{out}}(d^{\mu}_{\mathrm{s,r_1}} + d^{\mu}_{\mathrm{r_2,d}}) + \left[ABd^{\mu}_{\mathrm{r_1,r_2}}\gamma_{\mathrm{out}}\right]^{\frac{1}{2}}}, \tag{63}$$

$$P^{*}_{\mathrm{r_2,d}} = \frac{d^{\mu}_{\mathrm{r_2,d}}\gamma_{\mathrm{out}}P_{\mathrm{tot}}}{\gamma_{\mathrm{out}}(d^{\mu}_{\mathrm{s,r_1}} + d^{\mu}_{\mathrm{r_2,d}}) + \left[ABd^{\mu}_{\mathrm{r_2,d}}\gamma_{\mathrm{out}}\right]^{\frac{1}{2}}}. \tag{64}$$

The effectiveness of the derived optimal power allocation solutions will be verified in the following section where a numerical example which compares the system performance with and without power allocation is provided and discussed.

5 Simulation and numerical results

In this section, we validate the accuracy of the achieved analytical and asymptotic expressions via comparison with Monte Carlo simulations. Additionally, some numerical examples are provided and discussed to illustrate the impact of the number of available sources and order of selected source at the first hop, number of available destinations and order of selected destination at the third hop, and turbulence fading parameters and pointing errors on the system performance. The effectiveness of the proposed power allocation algorithm is also shown in this section. A total number of 2×10^5 samples/SNR value have been used in generating the simulation results. Also, the BPSK modulation scheme has been used in the results of ASEP.

The effect of the order of selected source at the first hop (N_1) and order of selected destination at the third hop (N_2) is illustrated in Fig. 2 for the case where $N_1 = N_2$. Excellent matching between the analytical and asymptotic results with Monte Carlo simulations can be seen in this figure. Also, it is clear that under weak turbulence conditions ($\alpha = 9.708$ and $\beta = 8.198$), as $N_1 = N_2$ decreases or, equivalently, as the quality of the selected source and destination enhances, better the achieved performance. This is because, for weak turbulence conditions, the system performance is dominated by both the first and third RF hops and hence, the diversity order of the system (G_d)

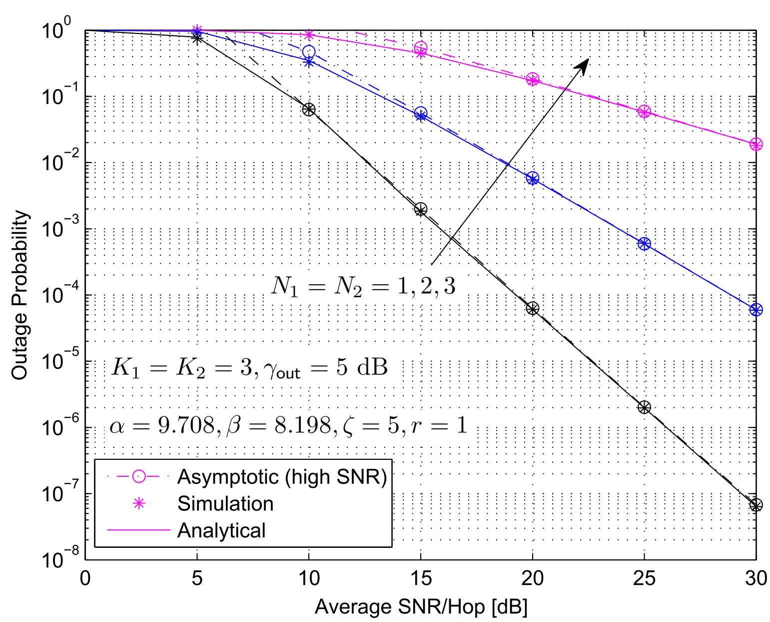

Fig. 2 P_{out} vs SNR of multiuser mixed RF/FSO/RF relay network with generalized order user scheduling for different values of $N_1 = N_2$

equals to $K_1 - N_1 + 1 = K_2 - N_2 + 1$. For fixed number of sources and destinations ($K_1 = K_2$), reducing $N_1 = N_2$ increases the diversity order of the system and enhances the system performance. For this case, the coding gain of the system (G_c) is expressed by the first case in (49).

Figure 3 portrays the outage behavior of the system under weak turbulence conditions for different numbers of sources and destinations when they are equal ($K_1 = K_2$). Again, it can be seen from this figure that the exact and asymptotic results perfectly match with the Monte Carlo simulations. Additionally, it is clear that under weak turbulence conditions ($\alpha = 9.708$ and $\beta = 8.198$), as $K_1 = K_2$ increases or, equivalently, the more the number of available sources and destinations, the better the achieved performance. This is because, for weak turbulence conditions, the system performance is dominated by both the first and third RF hops and hence, the diversity order of the system (G_d) equals to $K_1 - N_1 + 1 = K_2 - N_2 + 1$. For fixed order of selected source and destination ($N_1 = N_2$), increasing $K_1 = K_2$ increases the diversity order of the system and enhances the system performance. Again, the coding gain (G_c) for this case is expressed by the first case in (49). It is important to mention here that for both Figs. 2 and 3, the diversity order of the system is linearly proportional with the number of available sources and destinations and order of selected source and destination.

It is worth mentioning here that the issue of achieving the best performance and satisfying fairness among users is indeed a trade-off. The scheduling schemes which exist in literature can be divided according to two criteria: sum-rate capacity and fairness among users. Maximum rate or conventional scheduling maximizes the sum capacity of the system at the expense of fairness among users, whereas proportional fair user selection scheme satisfies fairness among users at the expense of system sum-rate [44, 45]. Therefore, the selection of the scheduling scheme depends on the system requirements and nature of the system. As an example on the suitability of the scheme to be used, although the proportional fair user scheduling could be helpful for users of weak channels, the loss that occurs in throughput when this scheduling scheme is used can be large in situations where users are scattered across the cell [46]. In summary, the opportunistic and even the generalized order user selection schemes are suitable for systems where the system overall sum-rate capacity or the overall performance is the main requirement of the system; conversely, the proportional fair user scheduling scheme is more desirable in systems where fairness among users is the first priority.

The outage performance vs SNR is portrayed in Fig. 4 under weak turbulence conditions ($\alpha = 8.650$ and $\beta = 7.142$) for different values of outage threshold γ_{out}. Two main cases are illustrated in this figure: the case where all links' average SNRs are increasing with increasing the x-axis value and the case where one of these SNRs is fixed. In the case where all SNRs are varying, the performance keeps enhancing as SNR increases and no noise floor appears in the results, whereas in the case where one SNR is kept fixed, a noise floor appears in the results, and a zero diversity order is achieved by the system. This behavior is expected as the system performance is dominated by the

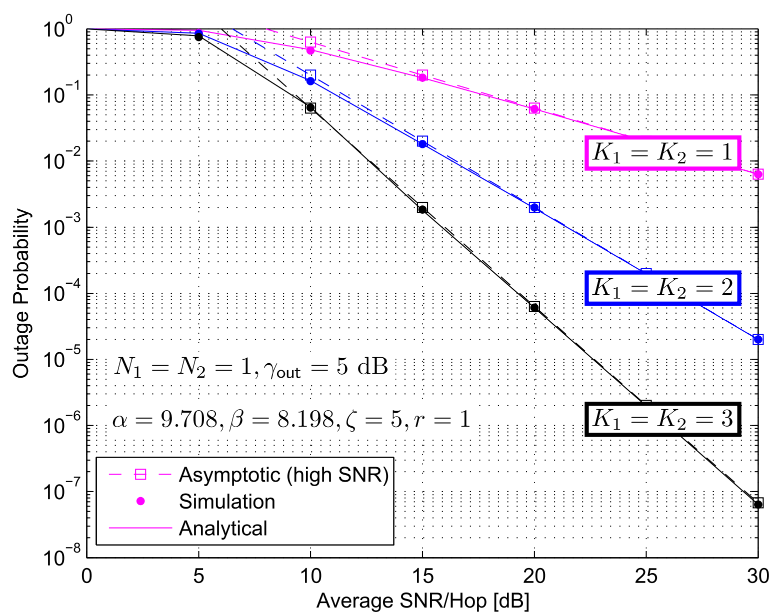

Fig. 3 P_{out} vs SNR of multiuser mixed RF/FSO/RF relay network with generalized order user scheduling for different values of $K_1 = K_2$

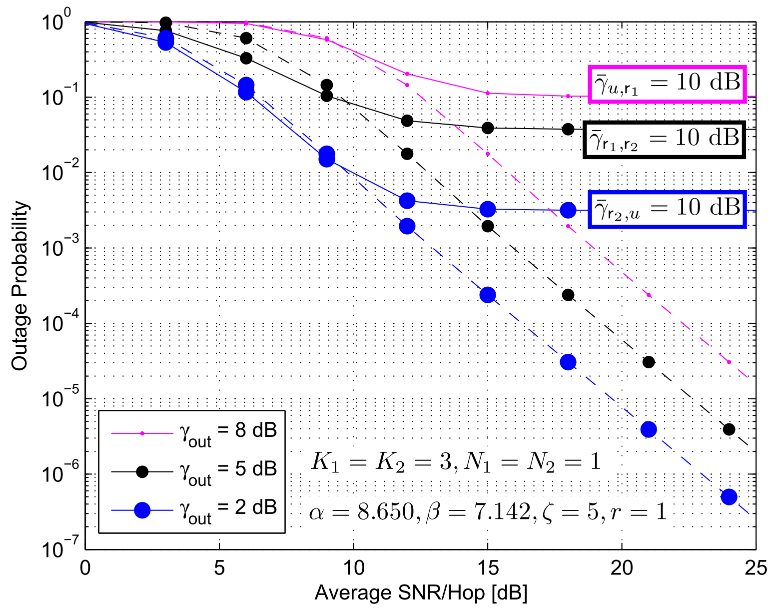

Fig. 4 P_{out} vs SNR of multiuser mixed RF/FSO/RF relay network with generalized order user scheduling for different values of γ_{out} with fixed average SNRs and varying average SNRs

worst link among the three links. It is clear also from this figure that in both cases, the outage threshold γ_{out} affects the system performance by only affecting its coding gain.

Figure 5 studies the outage performance of the system vs order of selected source/destination ($N_1 = N_2$) under weak turbulence conditions for different values of average SNR/hop. As expected, increasing $N_1 = N_2$ or, equivalently, decreasing the quality of the selected source and destination increases the outage probability and degrades the system performance. Also, it is obvious from this figure that the best performance is achieved at the largest value of SNR.

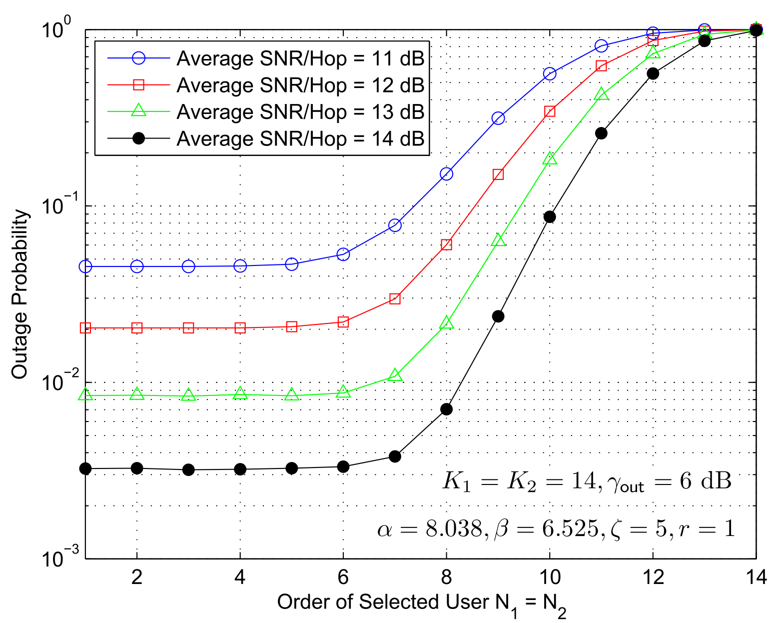

Fig. 5 P_{out} vs order of selected user of multiuser mixed RF/FSO/FSO relay network with generalized order user scheduling for different values of average SNR

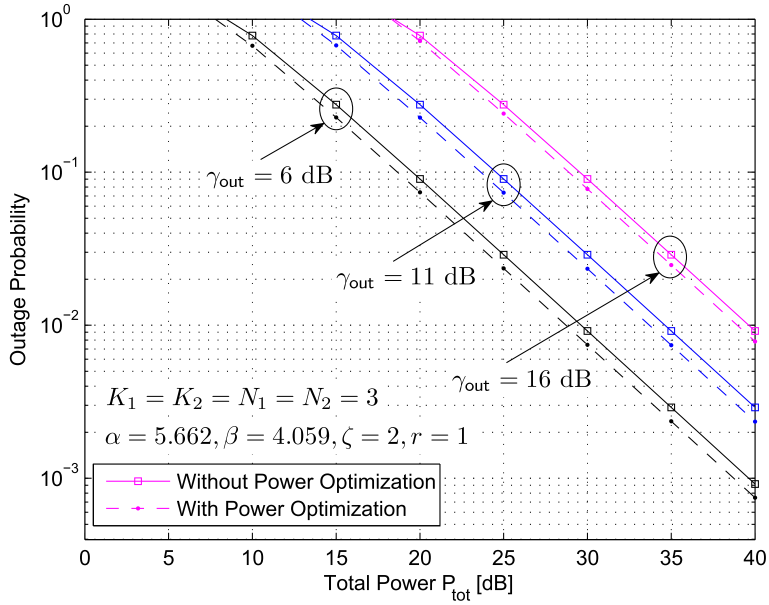

Fig. 6 P_{out} vs SNR of multiuser mixed RF/FSO/RF relay network with generalized order user scheduling for different values of γ_{out} without and with power optimization

The effectiveness of the proposed power allocation algorithm is illustrated in Fig. 6 under weak turbulence conditions for different values of outage threshold γ_{out}. Clearly, the system with optimum power allocation gives better performance compared to the case with no power allocation. Also, this figure shows that the outage threshold γ_{out} degrades the system performance through reducing the coding of the system and not the diversity order. This is in a full match with the asymptotic results which show that the outage threshold affects only the coding gain of the system. Note that in plotting this figure, the total distance (D_{tot}) between the sources and destinations was assumed to be 1 and divided between the three hops as follows: $D_{\text{s,r}_1} = 0.3$, $D_{\text{r}_1,\text{r}_2} = 0.3$, and $D_{\text{r}_2,\text{d}} = 0.4$.

Figure 7 studies the impact of pointing error, represented by ζ on the error probability performance of the

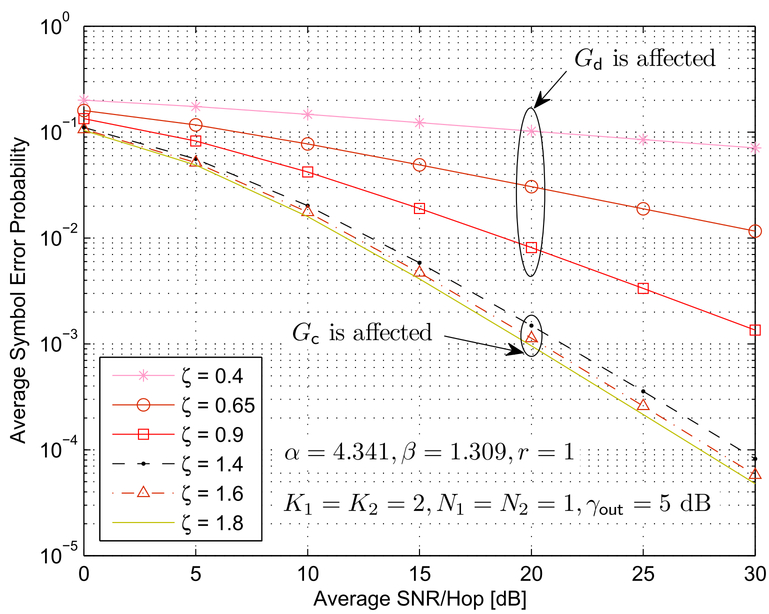

Fig. 7 ASEP vs SNR of multiuser mixed RF/FSO/RF relay network with generalized order user scheduling for different values of ζ

system under severe atmospheric turbulence conditions ($\alpha = 4.341$ and $\alpha = 1.309$). As the figure is generated for severe atmospheric turbulence conditions, the system performance will be dominated by the FSO link parameters (α, β and ζ^2). Based on the values of these three parameters, the curves in this figure could be divided into two sets: the set of curves where the diversity order (G_{d}) is affected by changing ζ and the set of curves where the coding gain (G_{c}) is affected by changing ζ. In the first case, the diversity order of the system is affected/determined by ζ^2 as it is the minimum parameter among α, β, and ζ^2. On the other hand, when the minimum value of these three parameters becomes equal β, changing ζ affects the coding gain of the system and not the diversity order which is in this case determined by β. This result is in a full match with the asymptotic result provided in the second part of (48). Note that in this figure, the type of the detector, represented by r, should also affect the diversity order of the system. It is assumed to be a heterodyne receiver with $r = 1$.

The two types of detection (heterodyne and IM/DD) are studied in Fig. 8, where the error probability performance is portrayed versus SNR under various atmospheric turbulence conditions. As expected, due to its ability to better overcome the thermal noise effect in the FSO systems, the heterodyne detection mode (i.e., $r = 1$) gives better results compared to the IM/DD detection mode (i.e., $r = 2$). This gain in the system performance is achieved at the expense of system complexity. For one type of detection, say $r = 1$ or $r = 2$, it is clear that under strong and medium atmospheric turbulence conditions, the system performance is dominated by the FSO link parameters and as the minimum value among the parameters (α, β, and ζ^2) which is β is almost constant, moving from strong to medium turbulence conditions is only affecting the coding gain of the system and not the diversity order. Whereas, moving from medium turbulence conditions to weak turbulence conditions makes the RF links dominate the system performance, where the diversity order equals $K_1 - N_1 + 1 = K_2 - N_2 + 1$. This new value for the diversity order is clearly larger than its value in the severe and medium turbulence conditions which explains why the system performance gets better under weak turbulence conditions compared to the other two cases.

Figure 9 illustrates more on the effect of the number of sources/destinations (K_1 and K_2) and order of selected sources/destinations (N_1 and N_2) on the error probability performance of the considered system. Two main cases are shown in this figure: severe atmospheric turbulence conditions ($\alpha = 4.341$ and $\beta = 1.309$) and weak atmospheric turbulence conditions ($\alpha = 6.993$ and $\beta = 5.460$). It is clear that under severe turbulence conditions ($\alpha = 4.341$ and $\beta = 1.309$), trying to increase $K_1 = K_2$ is not beneficial for the diversity order and coding gain of the system as they are determined by the FSO parameters that dominate the overall system performance. This case is represented by the brown and black curves on the figure. Whereas under weak turbulence conditions ($\alpha = 6.993$ and $\beta = 5.460$), it is obvious that the diversity order and coding gain of the system are dominated by the RF links parameters (K_1, N_1, K_2, and N_2). We can see that the diversity order of the system in this case is determined by

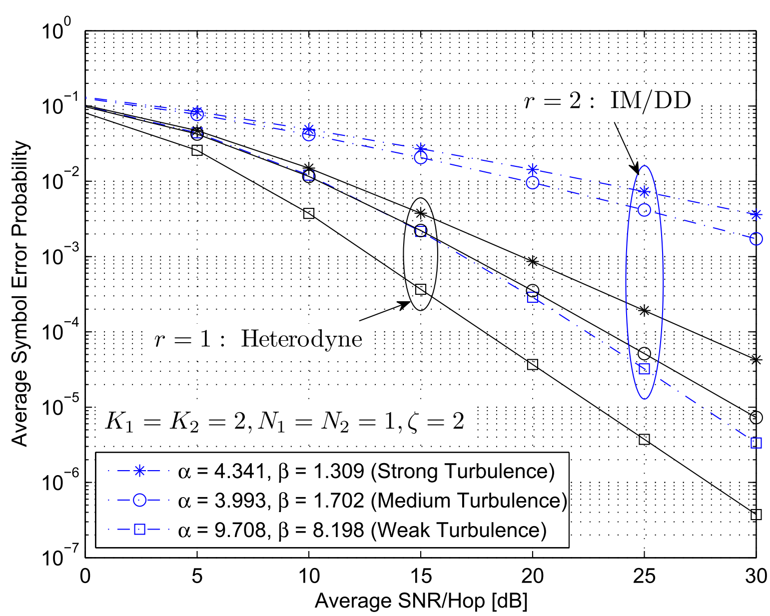

Fig. 8 ASEP vs SNR of multiuser mixed RF/FSO/RF relay network with generalized order user scheduling for different values of α, β, and r

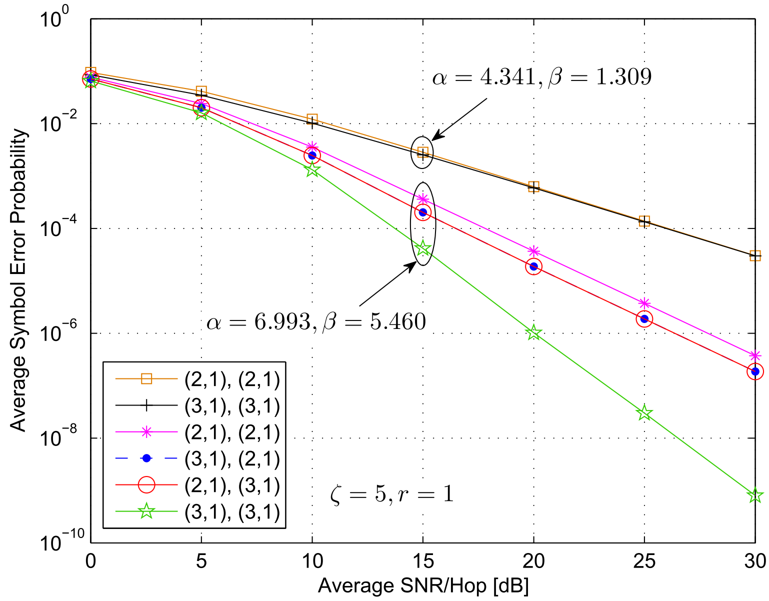

Fig. 9 ASEP vs SNR of multiuser mixed RF/FSO/RF relay network with generalized order user scheduling for different values of (K_1, N_1), and (K_2, N_2)

the minimum value among the terms $K_1 - N_1 + 1$ and $K_2 - N_2 + 1$. Keeping one term constant and increasing the other one enhances the coding gain of the system but not the diversity order. Finally, increasing both terms affects the minimum value among them and hence, increases the system diversity order as can be seen in the last curve in this figure (green-star curve).

The ergodic channel capacity versus SNR is plotted in Fig. 10 under weak atmospheric turbulence conditions for different values of $N_1 = N_2$. The gain achieved in the system capacity due to decreasing $N_1 = N_2$ or, equivalently, due to selecting a better source and destination is shown in this figure. This gain in the system performance is expected as enhancing the quality of the RF parts of the system is beneficial for the system performance under weak turbulence conditions. It is clear also from this figure that the analytical expressions are in excellent match with the simulation results.

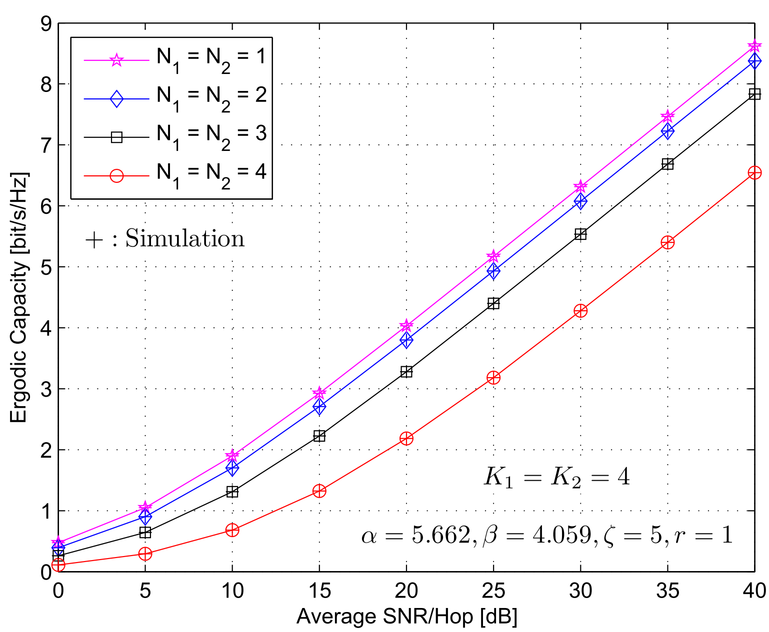

Fig. 10 Capacity vs SNR of multiuser mixed RF/FSO/RF relay network with generalized order user scheduling for different values of $N_1 = N_2$

6 Conclusions

In this paper, the performance of a new scenario of triple-hop multiuser mixed RF/FSO/RF relay network with generalized order user scheduling was evaluated. Also, a power allocation algorithm to calculate the optimum transmission power was proposed. Closed-form expressions were derived for the outage probability, average symbol error probability, and channel capacity assuming Rayleigh and Gamma-Gamma fading models for the RF and FSO links, respectively. The effect of pointing errors was also considered in the derivations. Furthermore, the system performance was studied at the high-SNR regime where an approximate expression for the outage probability, in addition to the diversity order and coding gain were provided. Monte Carlo simulations were provided to illustrate the validity of the achieved exact and asymptotic results. The main results illustrated that the system performance is dominated by the worst hop among the three hops. The diversity order and coding gain are determined by the parameters of the link/s which dominate the system performance. These parameters are: number of users and order of selected users in the RF links and atmospheric turbulence parameters, pointing error, and type of detector in the FSO link. Finally, the results showed that the proposed power allocation algorithm clearly enhances the system performance compared to the case with no power allocation.

Acknowledgements

This work was funded by the National Plan for Science, Technology and Innovation (Maarifah)—King Abdulaziz City for Science and Technology—through the Science and Technology Unit at the King Fahd University of Petroleum and Minerals (KFUPM)—the Kingdom of Saudi Arabia, under grant number 15-ELE4157-04.

Competing interests

The author declares that he has no competing interests.

Authors' information

Anas M. Salhab is a member of IEEE.

Received: 11 June 2016 Accepted: 6 October 2016
Published online: 28 October 2016

References

1. D Kedar, S Arnon, Urban optical wireless communications networks: the main challenges and possible solutions. IEEE Commun. Mag. **42**(5), 2–7 (2003)
2. ND Chatzidiamantis, HG Sandalidis, GK Karagiannidis, M Matthaiou, Inverse Gaussian modeling of turbulence-induced fading in free-space optical systems. IEEE/OSA J. Lightw. Technol. **29**(10), 1590–1596 (2011)
3. JN Laneman, DNC Tse, GW Wornell, Cooperative diversity in wireless networks: efficient protocols and outage behavior. IEEE Trans. Info. Theory. **50**(12), 3062–3080 (2004)
4. E Lee, J Park, D Han, G Yoon, Performance analysis of the asymmetric dual-hop relay transmission with mixed RF/FSO links. IEEE Photon. Technol. Lett. **23**(21), 1642–1644 (2011)
5. IS Ansari, F Yilmaz, M-S Alouini, Impact of pointing errors on the performance of mixed RF/FSO dual-hop transmission systems. IEEE Wirel. Commun. Lett. **2**(3), 351–354 (2013)
6. N Saquib, MSR Sakib, A Saha, M Hussain, in *Proc. Int. Conf. Education Technol. and Computer*. Free space optical connectivity for last mile solution in Bangladesh (IEEE, Shanghai, 2010), pp. 484–487
7. M Karimi, M Nasiri-Kenari, Outage analysis of relay-assisted free-space optical. IET Commun. **4**(12), 1423–1432 (2010). doi:10.1049/iet-com.2009.0335
8. P Puri, P Garg, M Aggarwal, Outage and error rate analysis of network-coded coherent TWR-FSO systems. IEEE Photon. Technol. Lett. **26**(18), 1797–1800 (2014)
9. BT Vu, TC Thang, AT Pham, in *Proc. 9th Int'l Symp. on Commun. Systems, Netw. and Digital Signal Process*. Selective relay decode-and-forward QAM/FSO systems over atmospheric turbulence channels (IEEE, Manchester, 2014), pp. 407–410
10. SI Hussain, MM Abdallah, KA Qaraqe, in *Proc. IEEE GCC Conf. and Exhibition*. Power optimization and *k*th order selective relaying in free space optical networks (IEEE, Doha, 2013), pp. 330–333
11. C Abou-Rjeily, Performance analysis of selective relaying in cooperative free-space optical systems. IEEE/OSA J. Lightw. Technol. **31**(18), 2965–2973 (2013)
12. ND Chatzidiamantis, GK Karagiannidis, On the distribution of the sum of Gamma-Gamma variates and applications in RF and optical wireless communications. IEEE Trans. Commun. **59**(5), 1298–1308 (2011)
13. J-Y Wang, J-B Wang, M Chen, X Song, Performance analysis for free-space optical communications using parallel all-optical relays over composite channels. IET Commun. **8**(9), 1437–1446 (2014). doi:10.1049/iet-com.2013.0754
14. IS Ansari, Yilmaz Fe, M-S Alouini, in *Proc. IEEE Veh. Technol. Conf*. On the performance of mixed RF/FSO variable gain dual-hop transmission systems with pointing errors (IEEE, Las Vegas, 2013), pp. 1–5
15. NI Miridakis, M Matthaiou, GK Karagiannidis, Multiuser relaying over mixed RF/FSO links. IEEE Trans. Commun. **62**(5), 1634–1645 (2014)
16. V Jamali, DS Michalopoulos, M Uysal, R Schober, in *Proc. IEEE Global Commun. Conf*. Mixed RF and hybrid RF/FSO relaying (IEEE, San Diego, 2015), pp. 1–6
17. B Makki, T Svensson, T Eriksson, M-S Alouini, in *Proc. IEEE Global Commun. Conf*. On the performance of HARQ-based RF-FSO links, (San Diego, 2015), pp. 1–7
18. B Makki, T Svensson, T Eriksson, M-S Alouini, On the performance of RF-FSO links with and without hybrid ARQ. IEEE Trans. Wirel. Commun. **15**(7), 4928–4943 (2016)
19. AM Salhab, F Al-Qahtani, RM Radaydeh, SA Zummo, H Alnuweiri, Power allocation and performance of multiuser mixed RF/FSO relay networks with opportunistic scheduling and outdated channel information. IEEE/OSA J. Lightw. Technol. **PP**(99) (2016). doi:10.1109/JLT.2016.2555944
20. AM Salhab, Performance of multiuser mixed RF/FSO relay networks with generalized order user scheduling and outdated channel information. Arabian J. Sci Eng. **40**(9), 2671–2683 (2015)
21. AA El-Malek, AM Salhab, SA Zummo, Security-reliability trade-off analysis for multiuser SIMO mixed RF/FSO relay networks with opportunistic user scheduling. IEEE Trans. Wireless Commun. **15**(9), 5904–5918 (2016)
22. PV Trinh, AT Pham, in *Proc. IEEE Veh. Technol. Conf*. Outage performance of dual-hop AF relaying systems with mixed MMW RF and FSO links (IEEE, Boston, 2015), pp. 1–5
23. I Stefan, H Haas, in *Proc. IEEE Veh. Technol. Conf*. Hybrid visible light and radio frequency communication systems (IEEE, Vancouver, 2014), pp. 1–5
24. M Kashef, M Ismail, M Abdallah, KA Qaraqe, E Serpedin, Energy efficient resource allocation for mixed RF/VLC heterogeneous wireless networks. IEEE J. Sel. Areas Commun. **34**(4), 883–893 (2016)
25. VK Sakarellos, CI Kourogiorgas, D Skraparlis, AD Panagopoulos, JD Kanellopoulos, End-to-end performance analysis of millimeter wave triple-hop backhaul transmission systems. Springer Wirel. Pers. Commun. **71**(4), 2725–2740 (2013)
26. SQ Nguyen, HY Kong, Outage performance and diversity analysis of cognitive triple-hop cluster-based networks under interference constraint. Springer Wirel. Pers. Commun. **85**(3), 1669–1688 (2015)
27. KP Peppas, CK Datsikas, Average symbol error probability of general-order rectangular quadrature amplitude modulation of optical wireless communication systems over atmospheric turbulence channels. J. Opt. Commun. Netw. **2**(2), 102–110 (2010)
28. WO Popoola, Z Ghassemlooy, BPSK subcarrier intensity modulated free-space optical communications in atmospheric turbulence. IEEE/OSA J. Lightw. Technol. **27**(8), 967–973 (2009)
29. J Park, E Lee, G Yoon, Average bit error rate of the Alamouti scheme in Gamma-Gamma fading channels. IEEE Photon. Technol. Lett. **23**(4), 269–271 (2011)

30. W Zhang, S Hranilovic, C Shi, Soft-switching hybrid FSO/RF links using short-length raptor codes: design and implementation. IEEE J. Sel. Areas Commun. **27**(9), 1698–1708 (2009)
31. B He, R Schober, Bit-interleaved coded modulation for hybrid RF/FSO systems. IEEE Trans. Commun. **57**(12), 3753–3763 (2009)
32. IS Gradshteyn, IM Ryzhik, *Tables of Integrals, Series and Products*, 6th ed. (Acadamic Press, San Diago, 2000)
33. TM Duman, A Ghrayeb, *Coding for MIMO Communication Systems*. (John Wiley & Sons, Ltd, Chichester, 2007). doi:10.1002/9780470724347
34. SS Ikki, S Aissa, A study of optimization problem for amplify-and-forward relaying over Weibull fading channels with multiple antennas. IEEE Commun. Lett. **15**(11), 1148–1151 (2011)
35. RJ Vaughan, WN Venables, Permanent expressions for order statistics densities. J. Roy. Statist. Soc. Ser. B. **34**(2), 308–310 (1972)
36. Wolfram, The Wolfram functions site (2013). http://functions.wolfram.com. Accessed Jan 2016
37. MR McKay, AL Grant, IB Collings, Performance analysis of MIMO-MRC in double-correlated Rayleigh environments. IEEE Trans. Commun. **55**, 497–507 (2007)
38. X Song, J Cheng, Optical communication using subcarrier intensity modulation in strong atmospheric turbulence. IEEE/OSA J. Lightwave Technol. **30**(22), 3484–3492 (2012)
39. A Farid, S Hranilovic, Outage capacity optimization for free-space optical links with pointing errors. IEEE/OSA J. Lightw. Technol. **25**(7), 1702–1710 (2007)
40. ND Chatzidiamantis, AS Lioumpas, GK Karagiannidis, S Arnon, in *Proc. IEEE Global Commun. Conf*. Optical wireless communications with adaptive subcarrier PSK intensity modulation (IEEE, Miami, 2010), pp. 1–6
41. IS Ansari, S Al-Ahmadi, F Yilmaz, M-S Alouini, H Yanikomeroglu, A new formula for the BER of binary modulations with dual-branch selection over generalized-K composite fading channels. IEEE Trans. Commun. **59**(10), 2654–2658 (2011)
42. MK Simon, M-S Alouini, *Digital Communication over Fading Channels*, 2nd ed. (John Wiley & Sons, Inc., Hoboken, 2005)
43. L Yang, X Gao, M-S Alouini, Performance analysis of relay-assisted all-optical FSO networks over strong atmospheric turbulence channels with pointing errors. IEEE/OSA J. Lightw. Technol. **32**(23), 4011–4018 (2014)
44. J-W So, JM Cioffi, Capacity and fairness in multiuser diversity systems with opportunistic feedback. IEEE Commun. Lett. **12**(9), 648–650 (2008)
45. L Yang, M Kang, M-S Alouini, On the capacity-fairness tradeoff in multiuser diversity systems. IEEE Trans. Veh. Technol. **56**(4), 1901–1907 (2007)
46. L Yang, M-S Alouini, in *Proc. IEEE Int. Conf. Commun*. Performance analysis of multiuser selection diversity (IEEE, Paris, 2004), pp. 3066–3070